An infectious virus-like particle built on a programmable icosahedral DNA framework

Yunyun Xu[1], Yuhe R. Yang[2,3], Qian Shi[1], Andrew B. Ward[3], Wei Wang[1], Yang Yang[1]*

[1]Institute of Molecular Medicine and Shanghai Key Laboratory for Nucleic Acid Chemistry and Nanomedicine, State Key Laboratory of Oncogenes and Related Genes, Renji Hospital, School of Medicine, Shanghai Jiao Tong University, Shanghai, 200127, China.

[2]National Center for Nanoscience and Technology, Chinese Academy of Sciences, Beijing, 100190, China

[3]Department of Integrative Structural and Computational Biology, The Scripps Research Institute, La Jolla, CA 92037

* Correspondence to: Yang.yang.nano@sjtu.edu.cn ORCID: 0000-0002-2630-6062

Abstract

Viral genomes can be compressed into a near spherical nanochamber to form infected particles. In order to mimic the virus morphology and packaging behavior, we invented a programmable icosahedral DNA nanoframe with enhanced rigidity and encapsulated the phiX174 bacteriophage genome. The packaging efficiency could be modulated through specific anchoring strands adjustment, and the enveloped phage genome remained accessible for enzymatic operations. Moreover, the packed complex could infect *E.* coli cells through bacterial uptake then produce plaques. This rigid icosahedral DNA architecture established a versatile platform to develop virus mimetic particles for convenient nucleic acid entrapment, manipulation and delivery.

Introduction

As the simplest “being”, virus, composed by nucleic acids, proteins and sometimes lipids, is considered an inevitable object in the path of understanding and defining life. Conventional microbiology, virology and molecular biology have paved the road of how to investigate viruses[1], meanwhile bioengineering has developed several neat and powerful tools to equip and utilize viruses (adenovirus vectors[2], phage display technology[3, 4], phage therapy[5], etc.), yet the mysteries and values of viruses haven’t been fully explored. The flourishing field of structural DNA nanotechnology offers strategies to assemble customized structures and organize individual molecules or particles with nanometer precision[6, 7, 8]. Besides employing DNA nanodevices to mimic[9, 10] or capture virus particles[11], a few examples have revealed that DNA nanostructures were competent in displaying and regulating viral proteins to study their assembly, infection efficiency and antigen induced immunity[12, 13, 14, 15]. These attempts suggest the opportunity of using artificial tools to dissect viruses, reorganize the components, investigate their behavior, functions and related biological mechanisms, and construct novel nano-devices for biomedical applications.

Among the critical processes in the virus life cycle (e.g. infection, replication, packaging and releasing), packaging as the last step of morphogenesis allows the maturation of the virion through protein-nucleotides interaction and end up with the micrometer long nucleic acid

winding inside a zeptoliter (10^{-12} nanoliter) tiny space[16]. Taking the well-studied ssDNA phage phiX174 as an example, along with the genome replication process, the 5386 nt ssDNA would recruit 60 copies of protein J, which is highly basic, to neutralize the charge and enter the procapsid[17, 18]. As a result, the phiX174 genome is packed inside the virion particle with a portion (8%~10%) of nucleotides immobilized in an icosahedral order at the inner surface of the protein shell[19, 20]. Acknowledging that the sophisticated near-spherical geometry and the inner decoration sites are key features of the virion for genome packaging during the matruation[21], we aim to manufacture an artificial DNA nanostructure to mimic the phiX174 packaging, explore strategies to densely load viral genome inside the structure and regulate the critical parameters of this process, and further polish the phage mimetic device for nucleic acid entrapment, engineering and delivery.

In this study, we constructed a rigid icosahedral DNA origami framework, equipped its inner surface with sufficient number of anchors, and enveloped the phiX174 genome inside the origami frame. The conditions for efficient packaging were systematically elaborated. We demonstrated that the hollow particle with regularly carved surface allowed the free entrance of enzymes to conduct molecular operations on the packed ssDNA. We further discovered that this mimetic complex solely composed of nucleic acid could passively infect the non-competent *E.* coli cells through bacterial uptake. The viral genome packaging strategy and the achieved phage mimetic nano device offers the opportunities for convenient phage engineering and delivery, which suggested multiple potentials in developing pseudo-phage therapy and nucleic acid vaccines. Meanwhile, the rigid and reliable icosahedral framework establishes a versatile platform that can be precisely functionalized, both inside and outside, to satisfy biochemical or biomedical researches with optimum modification and modulation.

Results

Nano frame assembly and ssDNA packaging

The icosahedral DNA origami frame (IDF) structure is designed via an open source software Tiamat. The IDF assembly is consist of a 7560 nt circular ssDNA scaffold which sequesters 216 staple strands (a.k.a. staples). The two dimensional (2D) blue print of the IDF illustrates the 30 edges of the icosahedron in an unfolded state (see Supplementary Figure 1). Each of the edge is designed as a four helix bundle with 63 nucleotides (~21 nm) in length. The four helices are considered as two layers of double-helix module, a foundation layer (FL) and an addition layer (AL). Scaffold strand at the foundation layer is applied to connect adjacent edges and route through the icosahedral frame, while a 126 nt scaffold loop protrudes from each edge and forms the addition layer with the assistance of staples (see Supplementary Figure 2). The IDF structure was successfully assembled through a 15 hour annealing program and purified with a rate-zonal gradient ultracentrifugation step[22]. The products were characterized by agarose gel electrophoresis (AGE) and negatively stained Transmission Electron Microscopy (nsTEM) (see Supplementary Figure 3). Structure models and representative nsTEM images of the natural phiX174 phage[20], the ssDNA genome, and the fabricated IDF structure were exhibited side by side in Figure 1a and 1b. The outstanding integrity and homogeneity of our IDF structure were attributed to the strengthened rigidity of the four helix bundle edges comparing to the 2 and 1 helix design published previously[13, 23, 24, 25]. The

topology of the IDF structure was further investigated through an orthogonal dimerization assay, in which, a pair of strands (termed a and a') with complementary sequences were protruded from either the foundation layer or the addition layer on one edge of the IDF. By mixing the four types of monomer structure (termed FL-a, FL-a', AL-a and AL-a') with one another, the clearly increased dimer bind intensity was observed only in the FL-a/FL-a' sample from the AGE image (see Supplementary Figure 4), which demonstrated that the IDF had its foundation layer facing outward and the addition layer facing inward. The two distinguishable faces are considered to be a result from the modified spacer at the vertices, compared to the previous design [26]. The staples crossing neighboring edges are linked by a 5T spacer (5nt polyT loop) in the foundation layer while a 1T spacer is introduced to the edge-crossing staples at the addition layer (see Figure 1b and Supplementary Figure 2). The slight differences in tension accumulated around the vertices between two layers determines the unidirectional folding of the structure. Thus, modifications on the inner or outer surface of the IDF can be distinguished and controlled.

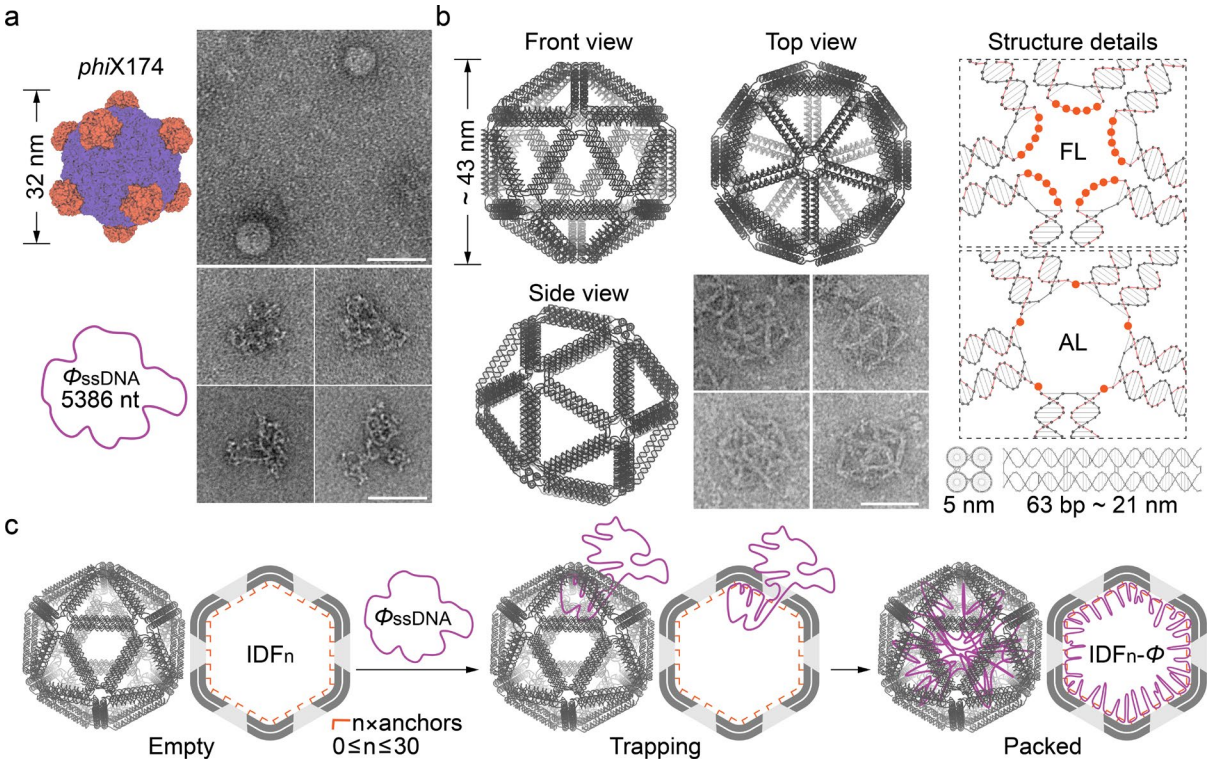

Figure 1. a. Structure model[20] and representative nsTEM images of the phiX174 phage particle and its ssDNA genome. b. Multi-view schemes of the IDF 3D model, representative nsTEM images of the assembled structure, and details of the IDF vertex (at both foundation layer and addition layer, each orange dot represented a T base) and edge. c. Hypothesized IDF induced phiX174 genome packaging process. Scale bar: 50 nm.

Next, the circular 5386 nt phiX174 genome (Φ_{ssDNA}) to be packaged inside the IDF nanoparticle was evenly divided into 30 fragments (29 × 180 nt + 1 × 166 nt), and the starting 10-30 nt of each section was chosen to be the anchoring site. Accordingly, the 30 edges of the IDF were re-assigned in an order following the Eulerian path with the shortest neighboring distance (see Supplementary Figure 5), thus 30 specific anchor sequences (complementary to the anchoring sites of the Φ_{ssDNA}) were sequentially allocated to the edges and protruded

from the addition layer towards the inner space of the IDF. As hypothesized in Figure 1c, once the Φ_{ssDNA} was mixed with the fully decorated icosahedron (termed IDF_{30}), the Φ_{ssDNA} might occasionally and partially stretch into the IDF from the triangular windows and get immobilized by the closest anchor strand with complementary sequence. Nucleated by the anchored sites, the probability of the anchoring events at the adjacent sites would be greatly increased due to the improved proximity between the anchors and their targeted segments. After a "domino-like" anchoring reaction, the whole genome was absorbed into the frame and fully packed as a nano complex IDF_{30}-Φ.

Considering the IDF_{30} as an enthalpy trap, the packaging efficiency would rely on the binding energy and kinetics, which resulted from the length of the anchor strands and the incubation conditions. By adjusting the anchor strand length from 10, 20 to 30 nt, three versions of IDF_{30} (e.g. IDF_{30}-10nt, -20nt, -30nt) were mixed with Φ_{ssDNA} at ratio 1:1 or 1:5 and incubated at different temperatures (e.g. room temperature ~23℃, 42℃ and 50℃) for the same amount of time (15 hrs). Results from the AGE analysis (see Supplementary Figure 6) suggested that the 10 nt anchor design was not strong enough to introduce or maintain the association between the Φ_{ssDNA} and the IDF_{30}, while frames with anchor length longer than 20 nt were sufficient in yielding products with slower mobility, moreover, higher temperatures would benefit the productivity. At 1:1 ratio, an emerged clear single band suggested a distinct product formation of IDF and Φ_{ssDNA} complex. An extra band and darker smears were observed at 1:5 ratio, which indicates dual or multiple ssDNA associated IDFs. Therefore, IDF_{30}-20nt was used to trap a Φ_{ssDNA} following the optimized protocol (see Supplementary Figure 6 and Methods section) in the following studies.

As shown in Figure 2a, the bare IDF without anchors (IDF_0) could hardly associate with Φ_{ssDNA}. In contrast, the IDF_{30}-20nt bound with Φ_{ssDNA} equivalently and efficiently, no further purification was performed. The achieved product IDF_{30}-Φ was subjected to nsTEM and Cryo-EM imaging (see Figure 2b and Supplementary Figure 7). From both type of EM images, IDF_{30}-Φ particles presented sharp and clear boundaries, similar to the bare IDF_{30}, but cloudier inner spaces. Single particle analysis (SPA) of the cryo-EM data provided higher resolution comparison of the empty and stuffed icosahedron frame with 2D classification and 3D reconstruction. Both the global and cross-section profiles of the 3D reconstruction of IDF_{30}-Φ exhibited extra interior electron density compared to the empty reference, which strongly suggested the successful packaging of Φ_{ssDNA} as hypothesized in Figure 1c. Moreover, the exterior of IDF_{30}-Φ and IDF_{30} provided equal level of electron density even at low threshold of the cryo-EM density maps (see Supplementary Figure 8). This observation indicated that the majority of Φ_{ssDNA} was trapped inside the IDF periphery, which could be attributed to the Mg^{2+} mediated charge neutralization and the intrinsic polymer properties of ssDNA (highly curled due to very short persistence length and end-to-end distance) [27, 28]. Furthermore, direct particle size measurement of the nsTEM images (EMI) and dynamic light scattering (DLS) analysis both proved that the particle sizes of IDF_{30} rarely changed after the packaging (see Figure 2c), which recurrently verified the outstanding rigidity of the IDF.

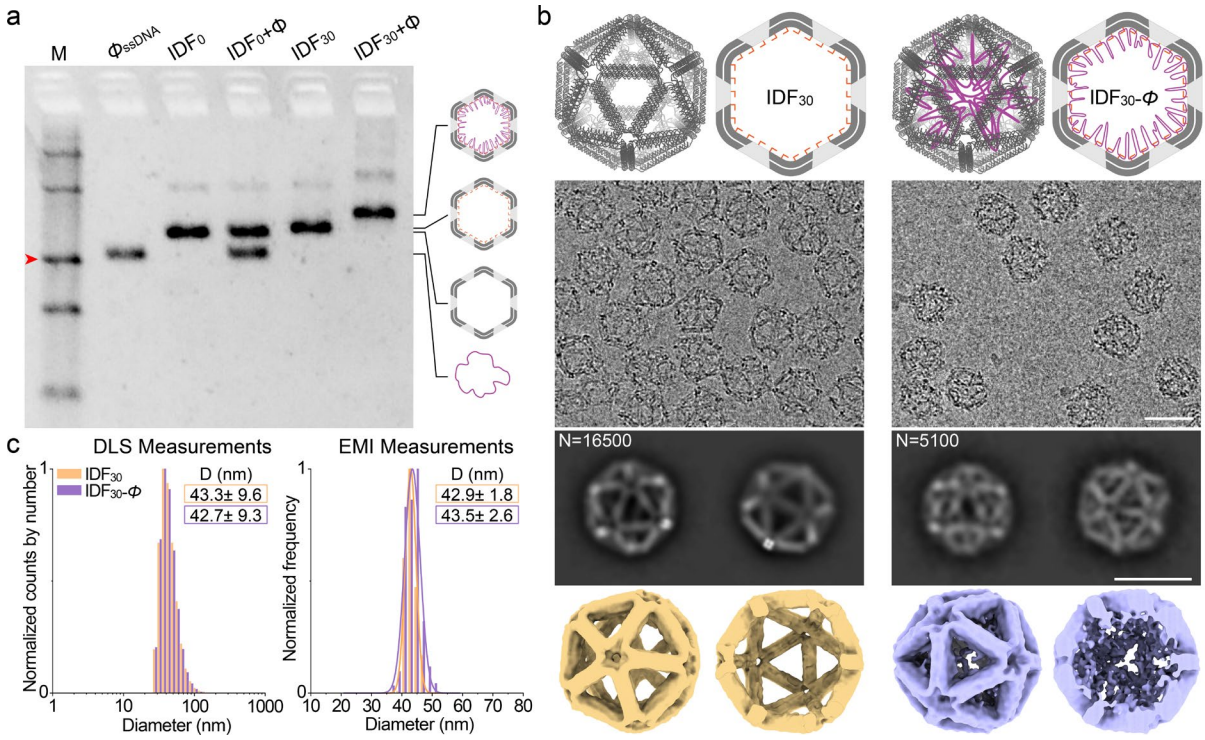

Figure 2. Characterization of ssDNA packaging. a. Φ_{ssDNA}, IDF_0, IDF_{30} and the products of ($IDF_{0\ or\ 30}$ + Φ_{ssDNA}) incubation characterized by agarose gel electrophoresis (1.5% AGE, 60V, 120 min, stained by GelRed; red arrow indicated the 1500 bp DNA marker band). b. CryoEM characterization of empty IDF_{30} particles and packed IDF_{30}-Φ complexes. 1st row: structure schemes; 2nd row: raw micrographs; 3rd row: representative images of the 2D classes and 4th row: 3D reconstruction results shown in global and cross-section mode. Scale bar: 50 nm. c. Statistics of the particle sizes from both dynamic light scattering analysis and electron microscopy imaging measurements.

To systematically investigate the packaging behavior, the number and position of anchor strands inside the IDF were precisely altered, taking the advantage of the full addressability of DNA origami structures[29]. IDFs with 18 and 6 anchors (named IDF_{18} and IDF_6) targeting evenly spaced segments of the Φ_{ssDNA} were assembled and examined by AGE (see Figure 3a). Band intensity analysis revealed that IDF_{18} packed Φ_{ssDNA} with 99.3% efficiency, whereas IDF_6 showed a slightly lower binding efficiency (91%) with two faint bands corresponding to the leftover IDF origami particles and ssDNAs. Interestingly, when 12 and 24 complementary strands (CS) with 20nt nucleotides each were co-assembled with IDF_{18}-Φ and IDF_6-Φ to compensate the anchor-missing segments along the Φ_{ssDNA}, the packing efficiencies could be recovered to near 100% and 93.2%, respectively. The visibly lagged IDF_6-Φ band (compare to IDF_{30}-Φ in the AGE gel image) indicated a less compact product, potentially due to the fact that the six long unbound ssDNA segments (~880 nt each) had higher chance to drift out of the frame which resulted in a slower mobility in the gel. Moreover, an IDF with only the front 10 anchors (IDF_{10}) targeting 1/3 of the Φ_{ssDNA} in an unbalanced distribution was assembled to test whether a partially packed product could be generated. The AGE analysis indicated that IDF_{10} and Φ_{ssDNA} also yielded a one-to-one associated complex with slower mobility and lower efficiency (similar to IDF_6-Φ) than IDF_{30}-Φ (see Figure 3b). Meanwhile, TEM images denoted that the IDF_{10}-Φ particles possessed a curled thread (ssDNA) tangling around the icosahedron,

which strongly supported the proposed packaging mechanism shown in Figure 1c.

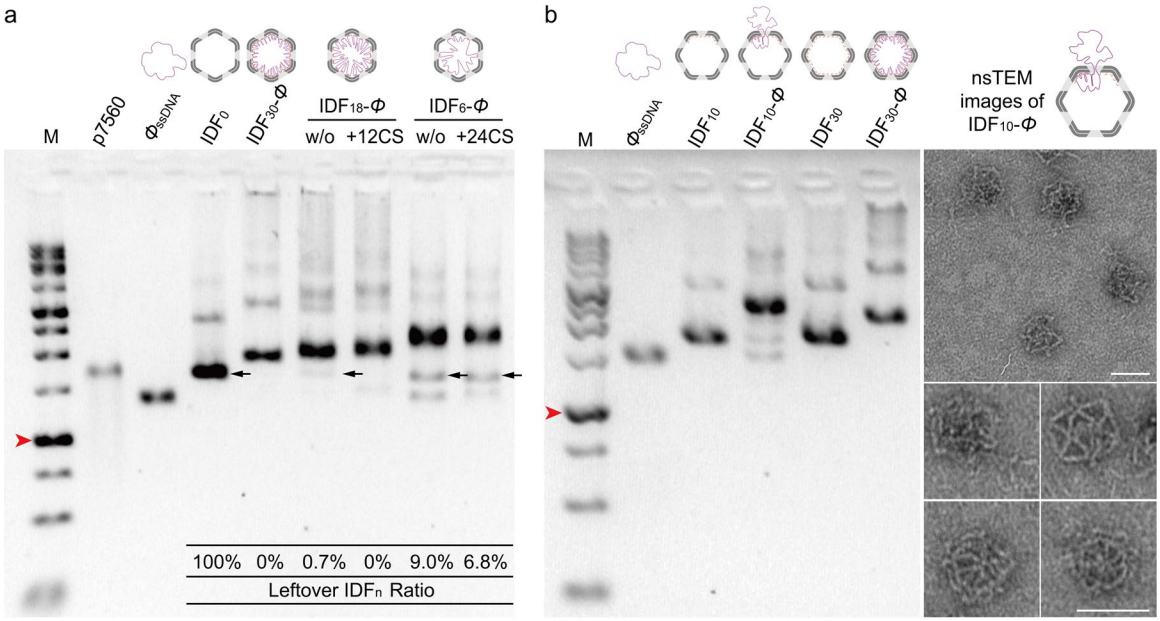

Figure 3. Packaging behavior modulation. a. AGE analysis of packaging products from IDF structures with 30, 18 or 6 evenly spaced anchoring strands, with or without compensate ssDNA oligos. Black arrows indicated the unpacked (leftover) IDF_n shells, and the ratio comparing to the starting material were calculated and listed at the bottom. b. AGE and nsTEM characterization of the IDF_{10} (continuously arranged instead of evenly spaced anchor strands) and Φ_{ssDNA} association. Red arrow indicated the 1000 bp DNA marker band. Scale bar: 50 nm.

Inner space accessibility and molecular operation

Different from the natural bacteriophage phiX174, whose genome is protected by the compact capsid with tightly assembled scaffold proteins, the inner space of the artificial IDF_n-Φ complex is accessible through the twenty regular triangle windows with 21 nm edge length. Thus, enzymatic reactions targeting the packed ssDNA are permitted. We first employed an ssDNA specific endonuclease, Mung bean nuclease (MBN), and tested whether it could enter IDF_{30}-Φ and digest the tethered Φ_{ssDNA}. AGE results clearly demonstrated that the molecular weight of IDF_{30}-Φ gradually decreased after the MBN treatment and reached the IDF_{30} level within 30 min digestion (see Figure 4a), indicating full digestion of the packaged Φ_{ssDNA}. While unpckaged free Φ_{ssDNA} was chopped into pieces in only 5 min at the same condition. Similar results were observed with P1 nuclease (see Supplementary Figure 9). Secondly, a classic rolling circle amplification (RCA) reaction using the packaged phiX174 circular ssDNA as templates was performed. Once the phi29 DNA polymerase and dNTP were mixed with IDF_{30}-Φ without the participation of additional primers, high molecular weight products were accumulated which stuck in the wells in AGE, along with the reduced band intensity of IDF_{30}-Φ. Samples after one-hour RCA reaction were examined by TEM, long ssDNA spread out of each icosahedron and mostly tangled into aggregates (see Figure 4b) were observed. Comparing to the free Φ_{ssDNA} templated RCA with 30 primers (20 nt each with the same

sequences of the anchor strands) included, where Φ_{ssDNA} was completely consumed in half an hour, the IDF_{30}-Φ was hardly exhausted in two hours. Therefore, it was convincing that the IDF packed ssDNA was accessible to other molecules in circumstances, but the enzymatic reactions were slowed down since diffusion of materials were likely to be limited with the DNA origami frame. Additionally, the operational RCA without additional primers indicated that the thirty anchor strands with available 3' hydroxide group would work as primers to amplify along the trapped Φ_{ssDNA} template, thus changing the number of anchor strands might result differently. To confirm this, IDF_{18}-Φ and IDF_6-Φ were applied to the RCA system, and it was obvious that the IDF particle with fewer anchors yielded more leftover structures after the two-hour reaction. Moreover, 12 and 24 extra primers were introduced to compensate the IDF_{18}-Φ and IDF_6-Φ complexes, respectively, for a total 30-primers formation, which recovered the RCA reaction with much less leftover products (see Supplementary Figure 10).

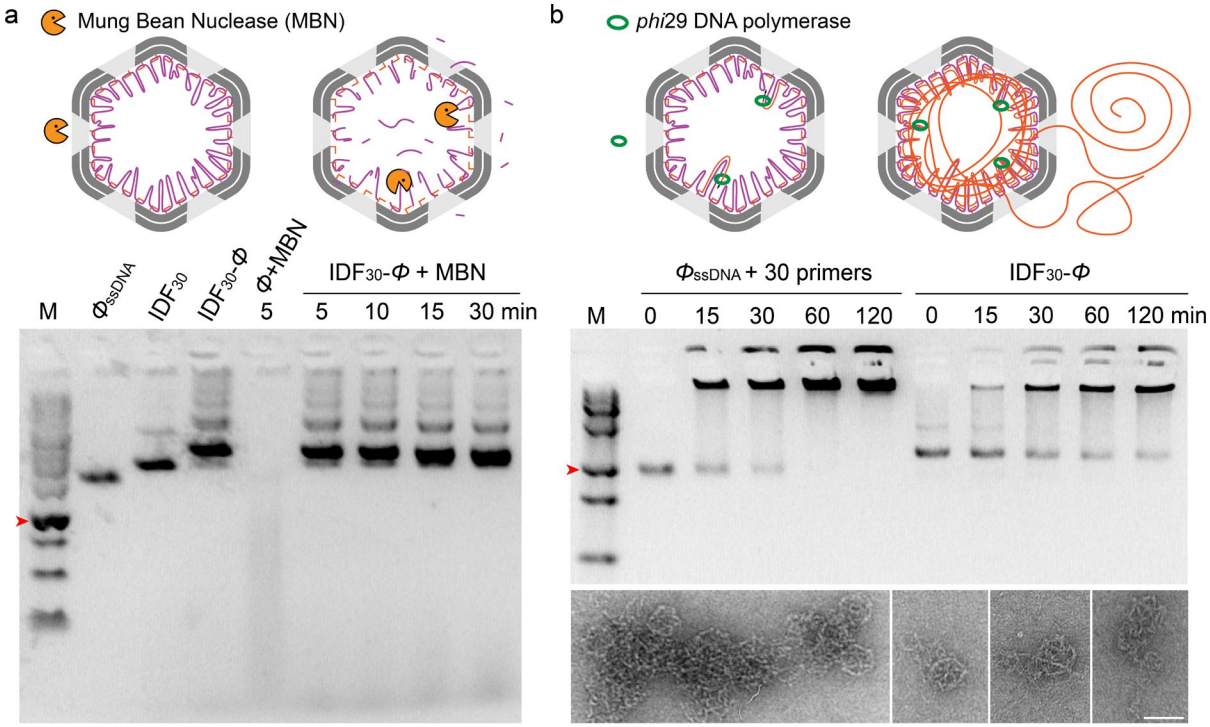

Figure 4. Accessible enzymatic reaction assays. a. scheme and AGE analysis of the MBN induced ssDNA digestion for both naked and packed phiX174 genome (red arrow indicates the 1000 bp DNA marker band). b. scheme and AGE analysis of the phi29 DNA polymerase induced RCA reaction (red arrow indicates the 1500 bp DNA marker band). Note that for naked Φ_{ssDNA}, 30 primers targeting the exact anchoring sites were added in 1:1 stoichiometry, while for IDF_{30}-Φ, no primers was involved. nsTEM images of the IDF_{30}-Φ sample after 60 min reaction were shown at the bottom row. Scale bar: 50 nm.

Host cell uptake induced passive infection

Although phiX174 genome was successfully packed in the artificial DNA nano frame in an icosahedral manner, the natural capability of phage infection was not expected to be inherited by the IDF_n-Φ complexes, in lack of the crucial protein components, such as the spike protein G and H[16, 30]. However, in attempts to verify the above prediction, significant amount of plaques were observed, surprisingly, upon mixing of *E.* coli C (a phiX174 sensitive strain of *E.* coli) with

IDF_{30}-*Φ* and cultured on agar plates, following the phage plaque assay protocol [31, 32] (see Methods section). It was noticeable that the plaque was only observed after 6 hours culturing at 37 ℃, which was much slower than the natural phiX174 infection[32] (normally 1~2 hours, see Supplementary Figure 11). This phenomenon was repeatedly confirmed, and the number of plaques followed a linear relationship with the IDF_{30}-*Φ* amount that was mixed with the cell, which led to a particle to plaque forming unit (pfu) ratio of 7.5×10^6 (See Supplementary Figure 12). The IDF particle could deliver the phiX174 genome into the bacteria cytoplasm; therefore direct the progress of real phage particle production and bacteria lysis. Whereas, comparing to the natural bacteriophage infection, whose particle to pfu ratio was normally close to one[33], the millions of times weaker IDF_{30}-*Φ* "infection" suggested a diverging internalization path. Meanwhile, the way of competent cell transformation was excluded, since the *E.* coli cells were treated at mid-log phase (OD_{600} at 0.2~0.8) without stimulation of electricity, bivalent cation, osmotic shock or heat shock[34]. Assuming that this passive infection process could be affected by the DNA to *E.* coli affinity, a few strategies aiming at modifying the IDF structure to improve the bacteria attachment were tested. By introducing oligolysine (K_n, n=6, 8, or 10) and polyethylene glycol conjugated oligolysine (PEG_{1K}-K_6) to the IDF_{30}-*Φ* to change its overall static potential[35], or by extending thirty DNA aptamer strands targeting *E.* coli[36] at the IDF_{30}-*Φ* outer surface to induce specific attachment, a vague hint of increased infection was observed (see Supplementary Figure 13), but solid conclusions could hardly be derived.

To better discover this mystery, a series of IDF_n-*Φ* complexes (n= 6, 18 and 30) were compared in parallel together with the naked $Φ_{ssDNA}$. Keeping the amount of added genome in constant (either packed or naked), the complex with more anchors generated more plaques in each trail, while the naked ssDNA accidentally resulted a few plaques (photos of a representative trail were shown in Figure 5a). To eliminate batch-to-batch differences, the counted plaque numbers were normalized by the IDF_{30}-*Φ* group in each trail and plotted with box analysis as shown in Figure 5b (see original data of each trial in Supplementary Figure 14). The trend of anchor number dependent plaque growth evidenced an essential role of the hybridized segments in the phage production process.

Based on the observations above, a possible scenario with detailed assumptions were stated as follows. Firstly, nucleic acid materials could enter the *E.* coli cytoplasm through cell uptake in a small but existing odds (comparing to competent cell transformation). As reported, in some naturally competent gram-negative bacteria species, the transformation of environmental dsDNA required particular pilus and associated transformation proteins to capture, predigest and transport the exogenous DNA[37, 38, 39]. Here, the assembled IDF particle probably entered the cell through different pathways, because the large size, particular geometry and high rigidity could hardly adapt to the transformation protein initiated internalization mechanism. Secondly, the IDF cage including the anchors might have helped the enveloped ssDNA bypass the immune (in other word, self-protection) system of *E.* coli *via* screening or delaying the associated enzymatic digestion. Thirdly, the internalized IDF particle allowed the entrance of bacterial DNA/RNA polymerase to accomplish the phiX174 mRNA transcription and genome amplification in a slower pace. Finally yet importantly, the anchor strands were believed participating the replication of the phage genome. The natural phiX174 genome replication were known to start with a discontinuously synthesis of the complementary (anti-sense) strand

to achieve a replicative form (RF) dsDNA, followed with a two-directional replication, and numerous gaps were reported existing on the complementary strand of the RF II molecules (nicking form *vs.* the supercoiled RF I form)[40]. Therefore, the IDF packed phiX174 genome with partially hybridized segments (with free 3' ends) unintentionally matched the pattern of the natural RF II DNA, and resulted the anchor number dependent plaque emergence. The proposed *E.* coli uptake induced passive infection process was shown in Figure 5c.

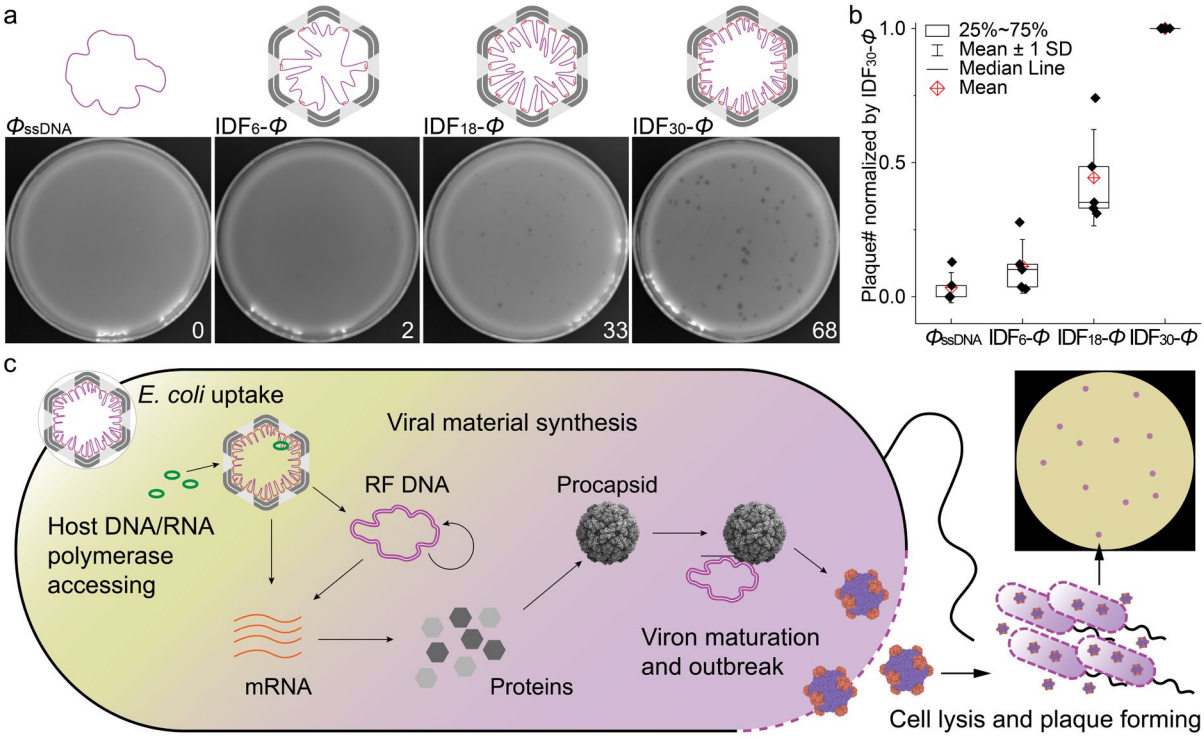

Figure 5. Mimetic particle infection study. a. a representative trail of plaque assay using naked or IDFn (n=6, 18 or 30) packed form of Φ_{ssDNA} to co-culture with *E.* coli C on arga plates. b. statistical analysis of five repeated trails of the plaque assay (original images and data shown in Supplementary Figure 15). c. Schematics of the proposed passive infection process initiated by bacterial uptake.

Discussion

As a general strategy, viral genome, the highly negatively charged DNA or RNA, could be packed into a near spherical protein shell nano compartment to form the infectious particle. One of the well-studied icosahedral fashioned virus nanoparticle is the bacteriophage phiX174. To mimic the phage morphology and packaging behavior, a *de novel* designed icosahedral DNA frame with reinforced rigidity was assembled. The direction of the folding is controlled with the unique two-layer design with different loop length at the vertices of each layer, therefore specific modification at either inner or outer surface has been achieved. By utilizing programmed anchoring strands that display over the inner surface of the IDF, the circular 5386nt natural phiX174 genome was efficiently packed into the DNA origami frame. Theoretically, this enthalpy trap strategy could be popularized to all sorts of wireframe cages with free excess[41, 42, 43, 44]. Yet, as a nature preferred geometry[21], the icosahedral framework was considered the optimum structure with high stability and sufficient anchoring sites for DNA

packaging. Meanwhile, stronger rigidity contributed by the two-layer design promoted the stability of the frame structure, the robustness of the packing process, as well as the reconstruction quality of the CryoEM characterization. These advantage was anticipated to keep benefiting future applications to use IDF origami platform as delivery machinery, nanoscaffold for EM based structural analysis, and nanoscaffold for in vivo therapeutics, etc. Moreover, not limited to ssDNA, single-stranded RNA in both circular and linear form could also fit in this packaging strategy. However, double-stranded DNA (dsDNA) as a general form of many viral genomes and plasmids, maintained a fully hybridized formation with high thermal stability and raised challenges for the IDF trapping. A few developed strategies that recruited particular binding agents (e.g. RecA protein[45], peptide nucleic acid (PNA)[46], transcription activator-like (TAL) effector proteins[47], etc.) to tag dsDNA at specific locations offered potential solutions for future In any case, the IDF structure could be expected to load nucleic acid materials of interest as a universal packaging framework.

Besides geometrical similarity endorsed and thermodynamically favored phage ssDNA packaging, the IDF particle showed unforeseen ability in delivering the packed phiX174 genome into the host bacterial cell and inducing phage outbreak. Without the participation of phage spike proteins or cell transformation conditions, this extraordinary infection was ascribed to passive bacterial uptake. Although the mechanism has not been fully discovered, the role of the IDF was speculated as a vehicle which could: 1) protect the packed ssDNA from digestion through bacterial internalization, 2) allow bacterial DNA and RNA polymerase to access the ssDNA to start the replication and transcription process, and 3) provide anchor strands as primers to initiate the synthesis of the anti-sense genome strand. Studies have yet to be done to reveal the IDF internalization pathway in various bacteria cells, which would highly enrich the potential applications of this artificial phage mimetic IDF structure in bacterial engineering.

This highly programmable, high yield, rigid and moderately permeable DNA icosahedral frame has more potential. With modifications on the inner surface, both imaging agents (e.g. fluorescent dyes and nanoparticles, nuclear magnetic resonance materials, radioactive isotopes, etc.) and drug molecules are permitted to load and enrich the inside of the frame with precise numbers and spatial arrangements. Even controllable molecule binding and releasing can be setup and implemented. Moreover, with modifications on the outer surface, this 3D framework could be equipped as an adequate vehicle towards cells by decorating specific recognition agents, such as DNA/RNA aptamers, antibodies, or viral spike proteins. Cell uptake efficiency has been proved to be affected by size, shape, rigidity and vertex curvature of DNA origami structures[48] , which indicated that our virus-like IDF structure has the potential to be an outstanding delivery device in developing the next generation of gene editing or nucleic acid vaccine strategy.

Methods

Folding and purification of the IDF structures

The icosahedral DNA origami frame (IDF) structure was designed by using Tiamat. To assemble the IDF structures, 7560 DNA scaffold was mixed with all necessary staple strands with 10× excess in the buffer composing of 1×TE and 10mM $MgCl_2$, with a final concentration

of 10 nM and total volume of 800 uL. The mixed solution was placed in a thermal cycler and underwent a 36 hours annealing process started at 75℃ for 5 mins and followed with a 65 to 4℃ programmed temperature ramp at a rate of -1℃/cycle × 60 cycles (36 min/cycle). The assembled structures were purified via a rate-zonal ultra-centrifugation process in glycerol gradients as described previously, concentrated by using Amicon Ultra centrifugal filters (30 kDa, 5min at 7500rpm and repeated three times to remove the extra glycerol) , and stored frozen at -20°C.

Agarose gel electrophoresis (AGE)

The concentration of purified DNA origami structures were quantified by A260 absorbance using Nanodrop One. Samples (normally 10 μL of 5 nM DNA origami) were applied on a1.5% agarose gel containing GelRed and run electrophoresis at 70 V for 1-2 hours at room temperature (running buffer: 0.5× TBE, 10 mM $MgCl_2$). Gel images were captured by the CCD equipped on the Amersham Imager 680 (AI680) instrument. Intensities of the interested bands were measured by an open source software ImageJ.

Negatively stained transmission electron microscopy (nsTEM)

All carbon-coated grids were first glow discharged to increase their hydrophilicity. 5 μl sample solution was placed on the grid surface and incubated for 1 min. Excess solution was adsorbed with filter paper. The grid was then washed by 5 μl 2% uranium acetate and stained by a second drop for 1 min. After removing the excess staining solution, the grid was left for air-dry. Imaging was performed using a Hitachi-HT7700 microscope operated at 100 kV.

Cryogenic temperature transmission electron microscopy (Cryo-TEM)

Cryo-TEM samples were adsorbed on glow-discharged holey carbon grids (Quantifoil MicroTools), then transferred to and frozen in liquid ethane using FEI Vitrobot. The specimen temperature was maintained below -170 °C during data collection. Cryo-EM imaging was performed on a Glacios TEM microscope, operated at 200 kV. To collect data for 3D reconstruction, the DNA icosahedron structure was derived from approximately 10,000 manually selected raw particle images. The microscope magnification was 57000x, corresponding to2.5 Å/pixel sampling at the specimen level.

Dynamic light scattering (DLS) measurement

Hydrodynamic diameter distribution of the IDF_{30} particles before and after Φ_{ssDNA} package were measured by dynamic light scattering using the Malvern Zetasizer ZS instrument, which was equipped with a 633 nm laser source and a backscattering detector.

The plaque assay

The purchased *E.* coli (freeze-dried powder) was added to 25ml LB liquid medium at 37°C, 200rpm shaker overnight to resuscitate. The recovered bacteria solution was added to LB liquid medium at ratio 1:100 and incubated for about 2 hours at 37°C (200rpm shaking), until the OD_{600} fell into the range of 0.2~0.8. 10 μL of the IDFn-Φ complex was mixed with 400μL bacteria solution and incubated for 30min at 37°C (200rpm shaking), then mixed with a pre-melted 4ml 0.5% agarose medium (cooled down and maintained at 37°C) and poured onto a

solid LB dish and incubated at 37°C for 6 hour. Plaques were manually counted with an error of ±5%.

Acknowledgement

This work was financially supported by Ministry of Science and Technology of China (2018YFA0902600), and National Natural Science Foundation of China grants (21977069). Bill and Melinda Gates Foundation and the Collaboration for AIDS Vaccine Discovery (CAVD), OPP1115782/INV-002916 (A.B.W.)

Author contributions

Y.X initiated the project, designed and performed most of the experiments, analyzed the data, and prepared the manuscript. Y.R.Y performed all the cryo-EM data analysis and prepared the manuscript. Q.S. participated to the structure design and assembly. A.B.W. supervised the cryo-EM data analysis and interpreted the data. W.W. supervised the bacteria infection study. Y.Y. initiated the project, designed the DNA origami structure and supervised the study, interpreted the data, and prepared the manuscript. All authors reviewed and approved the manuscript.

Competing financial interests

Authors declare the following competing financial interests: a provisional patent on the DNA-assisted liposome sorting method has been filed.

References

1. Bos L. 100 years of virology: from vitalism via molecular biology to genetic engineering. ***Trends Microbiol***, 8(2)**:** 82-87. **(2000)**

2. Altaras NE, Aunins JG, Evans RK, Kamen A, Konz JO, Wolf JJ. Production and formulation of adenovirus vectors. ***Adv Biochem Eng Biotechnol***, 99**:** 193-260. **(2005)**

3. Smith GP, Petrenko VA. Phage Display. ***Chem Rev***, 97(2)**:** 391-410. **(1997)**

4. Finlay WJ, Bloom L, Cunningham O. Phage display: a powerful technology for the generation of high specificity affinity reagents from alternative immune sources. ***Methods Mol Biol***, 681**:** 87-101. **(2011)**

5. Summers WC. Bacteriophage therapy. ***Annu Rev Microbiol***, 55**:** 437-451. **(2001)**

6. Yang Y, Zhang R, Fan C. Shaping Functional Materials with DNA Frameworks. ***Trends in Chemistry***, 2(2)**:** 137-147. **(2020)**

7. Seeman NC, Sleiman HF. DNA nanotechnology. ***Nat Rev Mater***, 3(1). **(2018)**

8. Hu Y, Niemeyer CM. From DNA Nanotechnology to Material Systems Engineering. ***Adv Mater***, 31(26)**:** e1806294. **(2019)**

9. Perrault SD, Shih WM. Virus-inspired membrane encapsulation of DNA nanostructures to achieve in vivo stability. ***ACS Nano***, 8(5)**:** 5132-5140. **(2014)**

10. Garmann RF, Sportsman R, Beren C, Manoharan VN, Knobler CM, Gelbart WM. A Simple RNA-DNA Scaffold Templates the Assembly of Monofunctional Virus-Like Particles. ***J Am Chem Soc***, 137(24)**:** 7584-7587. **(2015)**

11. Sigl C, Willner EM, Engelen W, Kretzmann JA, Sachenbacher K, Liedl A, Kolbe F, Wilsch F, Aghvami SA, Protzer U, Hagan MF, Fraden S, Dietz H. Programmable icosahedral shell system for virus trapping. ***Nat Mater***, 20(9)**:** 1281-1289. **(2021)**

12. Mikkila J, Eskelinen AP, Niemela EH, Linko V, Frilander MJ, Torma P, Kostiainen MA. Virus-encapsulated DNA origami nanostructures for cellular delivery. ***Nano Lett***, 14(4)**:** 2196-2200. **(2014)**

13. Veneziano R, Moyer TJ, Stone MB, Wamhoff EC, Read BJ, Mukherjee S, Shepherd TR, Das J, Schief WR, Irvine DJ, Bathe M. Role of nanoscale antigen organization on B-cell activation probed using DNA origami. ***Nat Nanotechnol***, 15(8)**:** 716-723. **(2020)**

14. Zhao Z, Zhang M, Hogle JM, Shih WM, Wagner G, Nasr ML. DNA-Corralled Nanodiscs for the Structural and Functional Characterization of Membrane Proteins and Viral Entry. ***J Am Chem Soc***, 140(34)**:** 10639-10643. **(2018)**

15. Zhou K, Ke Y, Wang Q. Selective in Situ Assembly of Viral Protein onto DNA Origami. ***J Am Chem Soc***, 140(26)**:** 8074-8077. **(2018)**

16. Denhardt DT, Model P. The Single-Stranded DNA Phages. ***CRC Critical Reviews in Microbiology***, 4(2)**:** 161-223. **(1975)**

17. Fujisawa H, Hayashi M. Viral DNA-synthesizing intermediate complex isolated during assembly of bacteriophage phi X174. ***J Virol***, 19(2)**:** 409-415. **(1976)**

18. Hafenstein S, Fane BA. phi X174 genome-capsid interactions influence the biophysical properties of the virion: evidence for a scaffolding-like function for the genome during the final stages of morphogenesis. ***J Virol***, 76(11)**:** 5350-5356. **(2002)**

19. McKenna R, Ilag LL, Rossmann MG. Analysis of the single-stranded DNA bacteriophage phi X174, refined at a resolution of 3.0 A. ***J Mol Biol***, 237(5)**:** 517-543. **(1994)**

20. McKenna R, Xia D, Willingmann P, Ilag LL, Krishnaswamy S, Rossmann MG, Olson NH, Baker TS, Incardona NL. Atomic structure of single-stranded DNA bacteriophage phi X174 and its functional implications. ***Nature***, 355(6356)**:** 137-143. **(1992)**

21. Dion MB, Oechslin F, Moineau S. Phage diversity, genomics and phylogeny. ***Nat Rev Microbiol***, 18(3)**:** 125-138. **(2020)**

22. Lin C, Perrault SD, Kwak M, Graf F, Shih WM. Purification of DNA-origami nanostructures by rate-zonal centrifugation. ***Nucleic Acids Res***, 41(2)**:** e40. **(2013)**

23. Banerjee A, Bhatia D, Saminathan A, Chakraborty S, Kar S, Krishnan Y. Controlled release of encapsulated cargo from a DNA icosahedron using a chemical trigger. ***Angew Chem Int Ed Engl***, 52(27)**:** 6854-6857. **(2013)**

24. Bhatia D, Mehtab S, Krishnan R, Indi SS, Basu A, Krishnan Y. Icosahedral DNA nanocapsules by modular assembly. ***Angew Chem Int Ed Engl***, 48(23)**:** 4134-4137. **(2009)**

25. Knappe GA, Wamhoff EC, Read BJ, Irvine DJ, Bathe M. In Situ Covalent Functionalization of DNA Origami Virus-like Particles. ***ACS Nano***, 15(9)**:** 14316-14322. **(2021)**

26. Zhang F, Jiang S, Wu S, Li Y, Mao C, Liu Y, Yan H. Complex wireframe DNA origami nanostructures with multi-arm junction vertices. ***Nat Nanotechnol***, 10(9)**:** 779-784. **(2015)**

27. Tinland B, Pluen A, Sturm J, Weill G. Persistence Length of Single-Stranded DNA. ***Macromolecules***, 30(19)**:** 5763-5765. **(1997)**

28. Rivetti C, Walker C, Bustamante C. Polymer chain statistics and conformational analysis of DNA molecules with bends or sections of different flexibility. ***J Mol Biol***, 280(1)**:** 41-59. **(1998)**

29. Rothemund PW. Folding DNA to create nanoscale shapes and patterns. ***Nature***, 440(7082)**:** 297-302. **(2006)**

30. Sun L, Young LN, Zhang X, Boudko SP, Fokine A, Zbornik E, Roznowski AP, Molineux IJ, Rossmann MG, Fane BA. Icosahedral bacteriophage PhiX174 forms a tail for DNA transport during infection. ***Nature***, 505(7483)**:** 432-435. **(2014)**

31. Anderson B, Rashid MH, Carter C, Pasternack G, Rajanna C, Revazishvili T, Dean T, Senecal A, Sulakvelidze A. Enumeration of bacteriophage particles: Comparative analysis of the traditional plaque assay and real-time QPCR- and nanosight-based assays. ***Bacteriophage***, 1(2)**:** 86-93. **(2011)**

32. Slattery SD, Valentine CR. Development of a microplate assay for the detection of single plaque-forming units of bacteriophage PhiX174 in crude lysates. ***Environ Mol Mutagen***, 41(2)**:** 121-125. **(2003)**

33. McCormick W, Mermel LA. The basic reproductive number and particle-to-plaque ratio: comparison of these two parameters of viral infectivity. ***Virol J***, 18(1)**:** 92. **(2021)**

34. Mercenier A, Chassy BM. Strategies for the development of bacterial transformation systems. ***Biochimie***, 70(4)**:** 503-517. **(1988)**

35. Ponnuswamy N, Bastings MMC, Nathwani B, Ryu JH, Chou LYT, Vinther M, Li WA, Anastassacos FM, Mooney DJ, Shih WM. Oligolysine-based coating protects DNA nanostructures from low-salt denaturation and nuclease degradation. ***Nat Commun***, 8**:** 15654. **(2017)**

36. Mela I, Vallejo-Ramirez PP, Makarchuk S, Christie G, Bailey D, Henderson RM, Sugiyama H, Endo M, Kaminski CF. DNA Nanostructures for Targeted Antimicrobial Delivery. ***Angew Chem Int Ed Engl***, 59(31)**:** 12698-12702. **(2020)**

37. Chen I, Dubnau D. DNA uptake during bacterial transformation. ***Nat Rev Microbiol***, 2(3)**:** 241-249. **(2004)**

38. Dubnau D, Blokesch M. Mechanisms of DNA Uptake by Naturally Competent Bacteria. ***Annu Rev Genet***, 53**:** 217-237. **(2019)**

39. Mell JC, Redfield RJ. Natural competence and the evolution of DNA uptake specificity. ***J Bacteriol***, 196(8)**:** 1471-1483. **(2014)**

40. Eisenberg S, Denhardt DT. Structure of nascent phiX174 replicative form: evidence for discontinuous DNA replication. ***Proc Natl Acad Sci U S A***, 71(3)**:** 984-988. **(1974)**

41. Benson E, Mohammed A, Gardell J, Masich S, Czeizler E, Orponen P, Hogberg B. DNA rendering of polyhedral meshes at the nanoscale. ***Nature***, 523(7561)**:** 441-444. **(2015)**

42. Veneziano R, Ratanalert S, Zhang K, Zhang F, Yan H, Chiu W, Bathe M. Designer nanoscale DNA assemblies programmed from the top down. ***Science***, 352(6293)**:** 1534. **(2016)**

43. Han D, Pal S, Yang Y, Jiang S, Nangreave J, Liu Y, Yan H. DNA gridiron nanostructures based on four-arm junctions. ***Science***, 339(6126)**:** 1412-1415. **(2013)**

44. Zhang Z, Yang Y, Pincet F, Llaguno MC, Lin CX. Placing and shaping liposomes with reconfigurable DNA nanocages. ***Nat Chem***, 9(7)**:** 653-659. **(2017)**

45. Sharma R, Davies AG, Walti C. RecA protein mediated nano-scale patterning of DNA scaffolds. ***J Nanosci Nanotechnol***, 11(12)**:** 10629-10632. **(2011)**

46. Muller P, Rossler J, Schwarz-Finsterle J, Schmitt E, Hausmann M. PNA-COMBO-FISH: From combinatorial probe design in silico to vitality compatible, specific labelling of gene targets in cell nuclei. ***Exp Cell Res***, 345(1)**:** 51-59. **(2016)**

47. Praetorius F, Dietz H. Self-assembly of genetically encoded DNA-protein hybrid nanoscale shapes. ***Science***, 355(6331). **(2017)**

48. Hu Q, Wang S, Wang L, Gu H, Fan C. DNA Nanostructure-Based Systems for Intelligent Delivery of Therapeutic Oligonucleotides. ***Adv Healthc Mater***, 7(20)**:** e1701153. **(2018)**

Supplementary Information

An infectious virus-like particle built on a programmable icosahedral DNA framework

Yunyun Xu, Yuhe R. Yang, Qian Shi, Andrew B. Ward, Wei Wang, Yang Yang

Contents

Structure design

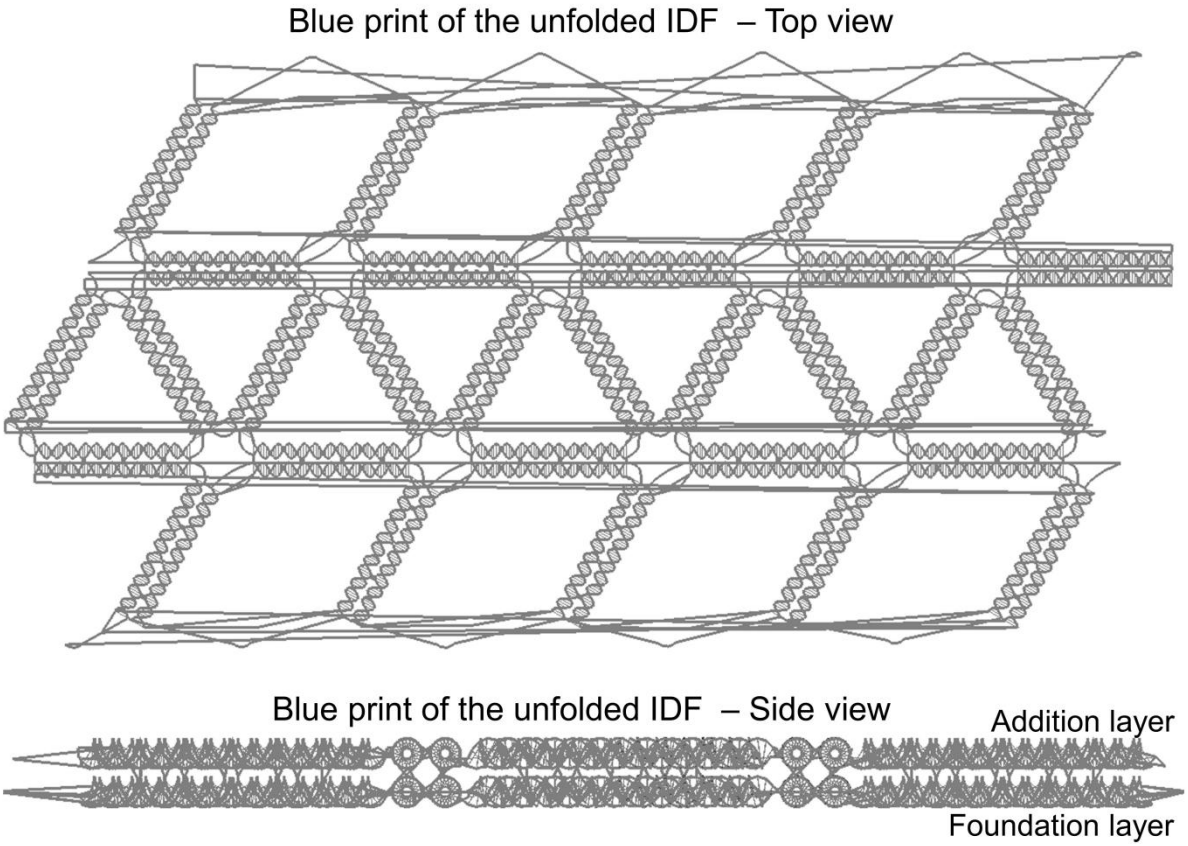

Figure S1. Blue print of the unfolded icosahedral DNA framework designed by Tiamat.

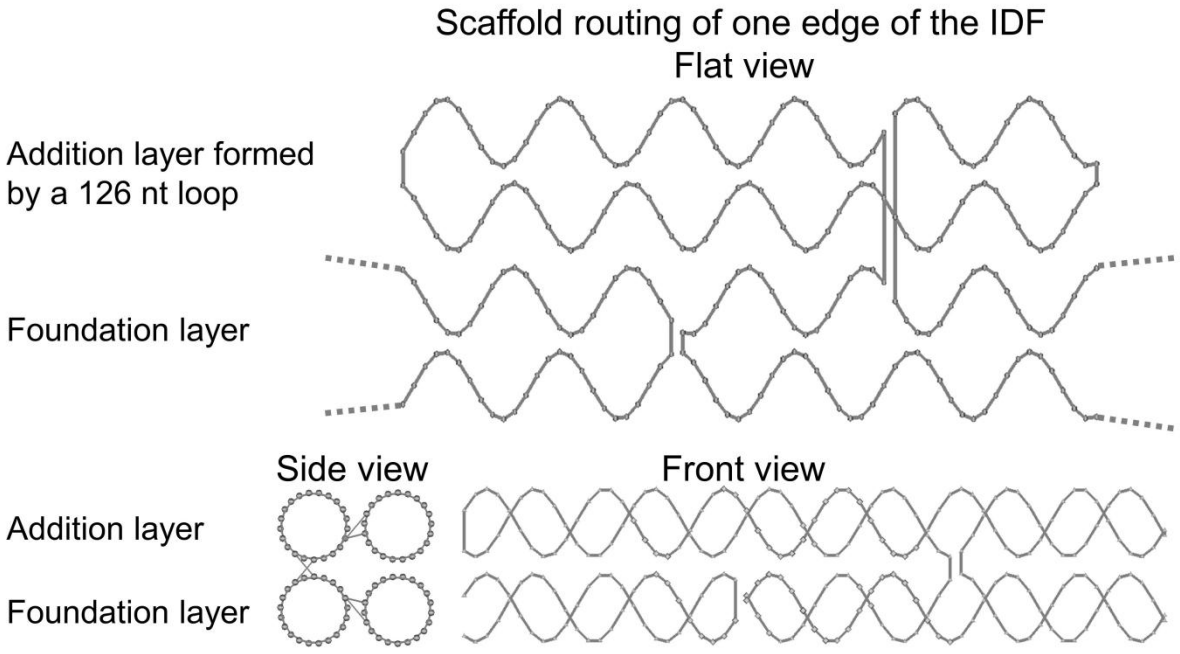

Figure S2. Details of the scaffold routing design on one edge. Top: the four helixes of the edge were arranged in an un-overlapped flat view to show the relationship between the addition layer and the foundation layer. Bottom: the side view and front view of the exampled edge at overlapped state. Note that all the staple strands were removed from this scheme to better exhibit the scaffold routing.

Results

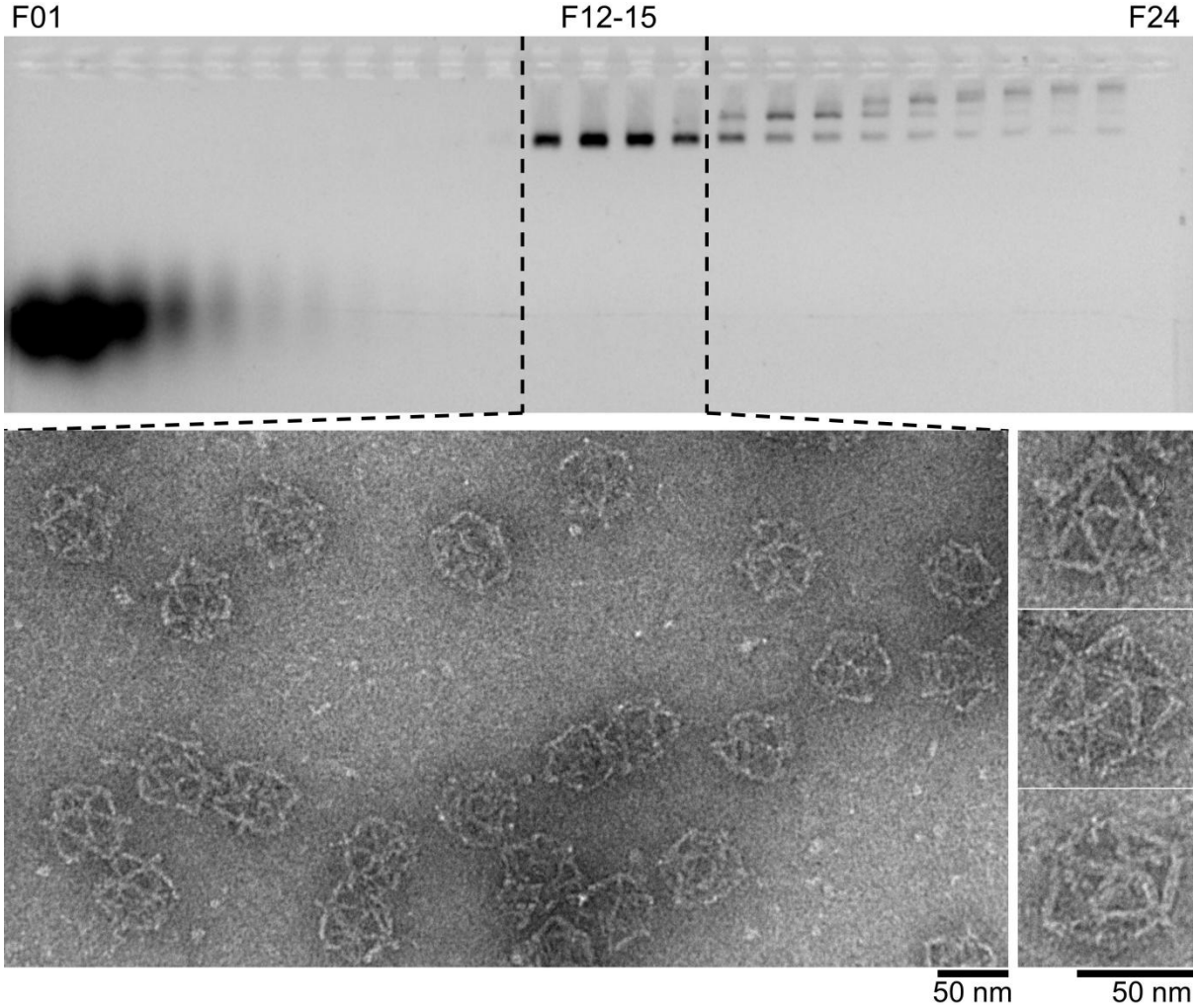

Figure S3. IDF structure purification and characterization. Top: representative agarose gel image of the ultracentrifugation products of an IDF_0 sample. Fractions 1–24 were collected from the top to the bottom of the glycerol gradient. F1-7 contained most of the extra staple strands, F12-15 contained only well assembled monomer IDF (combined for future use), and later fractions contained byproducts such as higher order structures and aggregates. Bottom: nsTEM images of the purified IDF_0 structure recovered from F12-15.

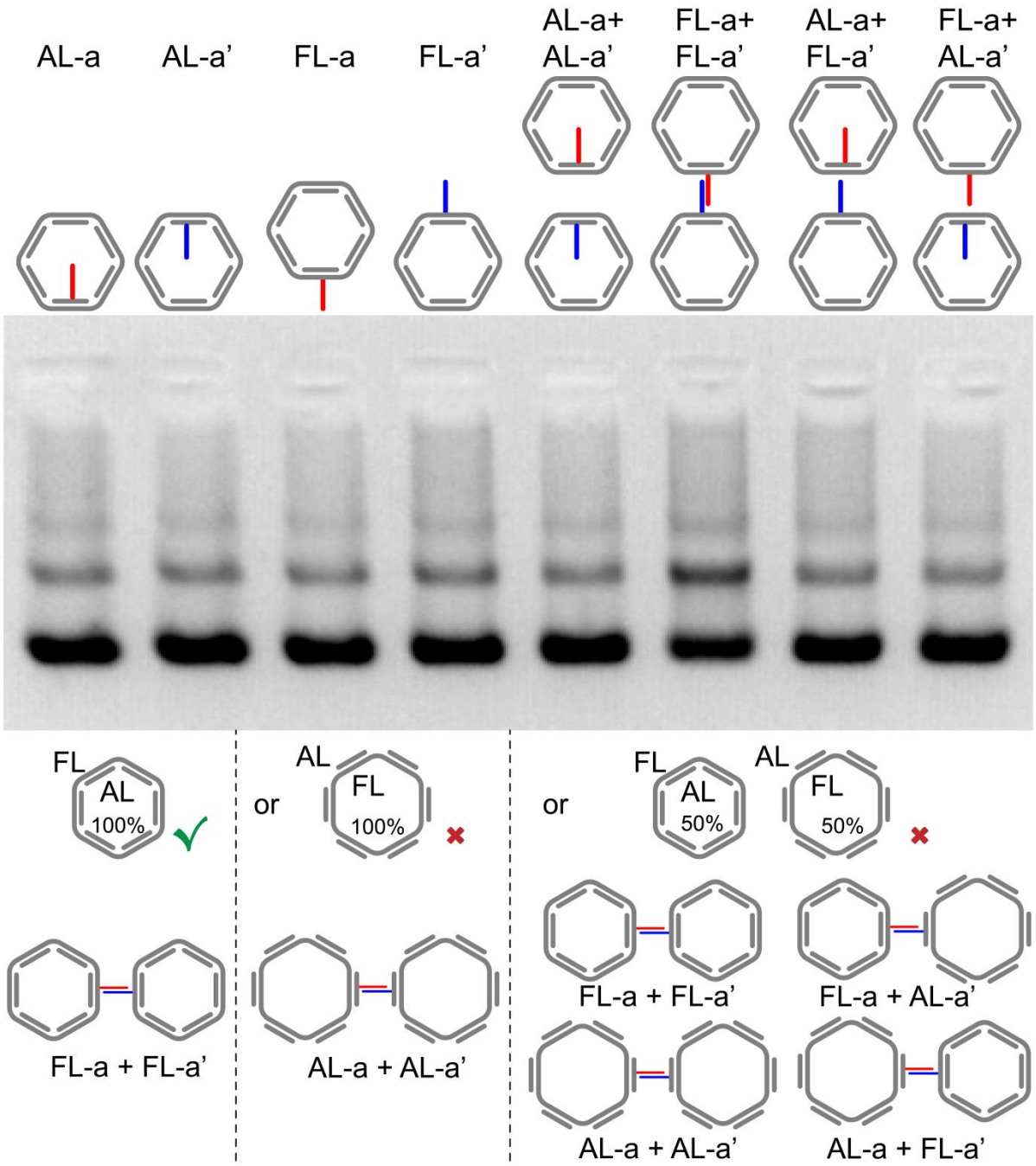

Figure S4. Verification of the structure topology. As shown in the top panel, four types of IDF variants with a or a' handle sequence protruding from the addition layer or the foundation layer were assembled and purified. The monomers were mixed with each other at 1:1 ratio followed with a one hour incubation at 37℃. All of the eight samples were applied to agarose gel electrophoresis, and only sample FL-a +FL-a' yielded an increased dimer band intensity. Bottom panel listed all the possible topological preferences with their achievable dimer species. AGE image indicated that the IDF structure folded its addition layer towards the inside while the foundation layer facing outside of the icosahedron.

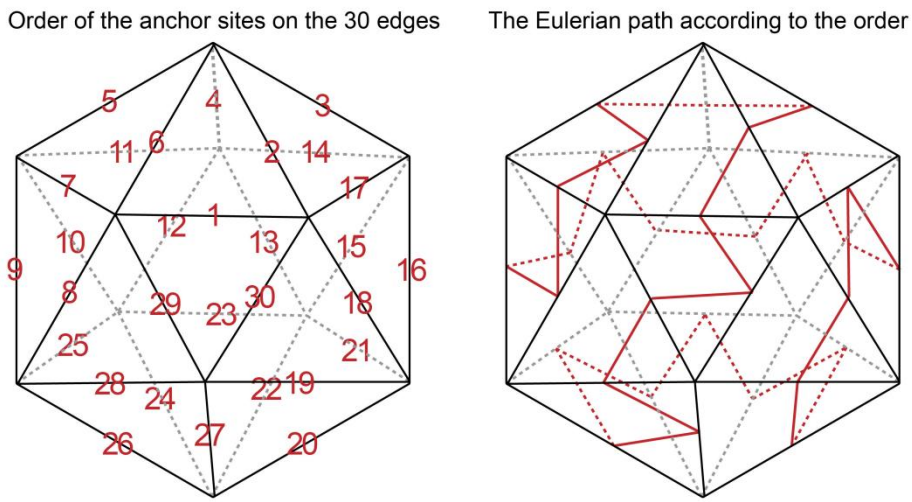

Figure S5. Arrangement of the anchor sites. The 30 edges of the IDF structure were assigned with numbers (left) following the Eulerian order which assured the shortest length between adjacent numbers (right). 30 anchor strands targeting the Φ_{ssDNA} were protruded from the staples on the addition layer of edges following the defined order.

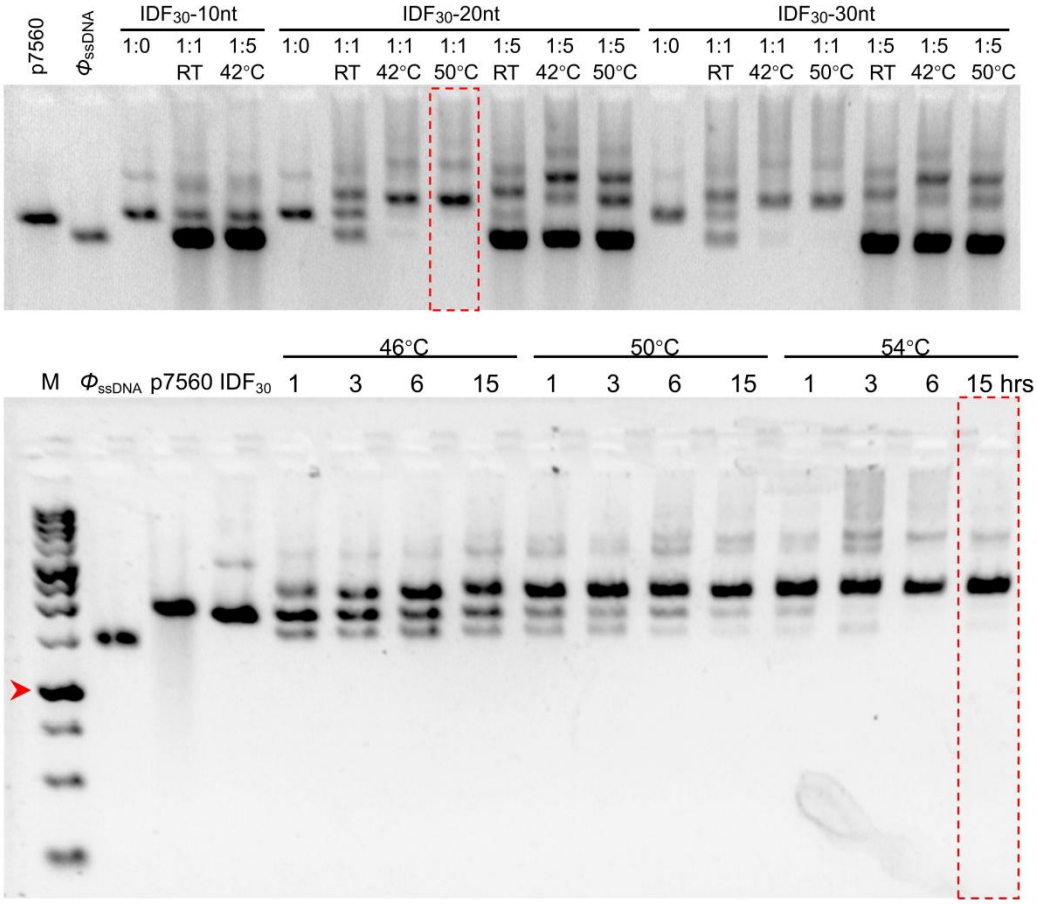

Figure S6. Optimization of the Φ_{ssDNA} packaging conditions with AGE analysis. Top: comparison of the packaging efficiency with varied anchor strand lengths, IDF_{30} to Φ_{ssDNA} ratios, and temperatures for an overnight (>18hrs) thermostatic incubation. Bottom: with the 20nt anchor and the 1:1 ratio fixed, the incubation temperature and lasting time were further examined. Dashed red boxes showed the results at the best conditions, in which both the IDF_{30} and the Φ_{ssDNA} bands vanished while a single product band with slower mobility emerged. Red arrow indicates the 1000 bp DNA marker band.

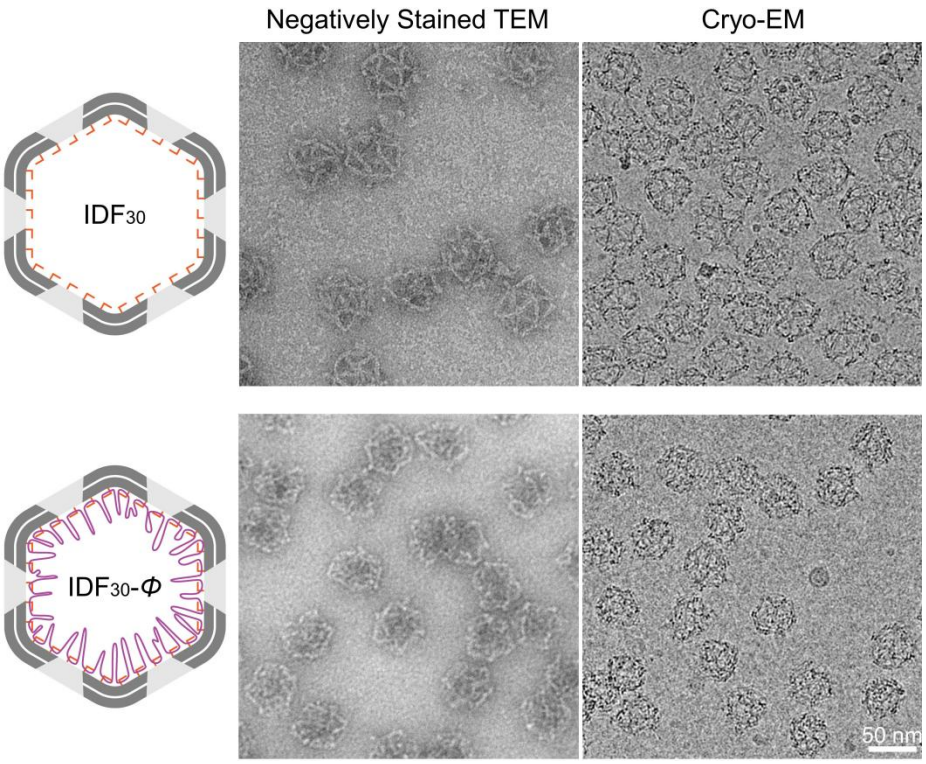

Figure S7. Representative nsTEM and CryoEM images of both IDF_{30} and IDF_{30}-Φ.

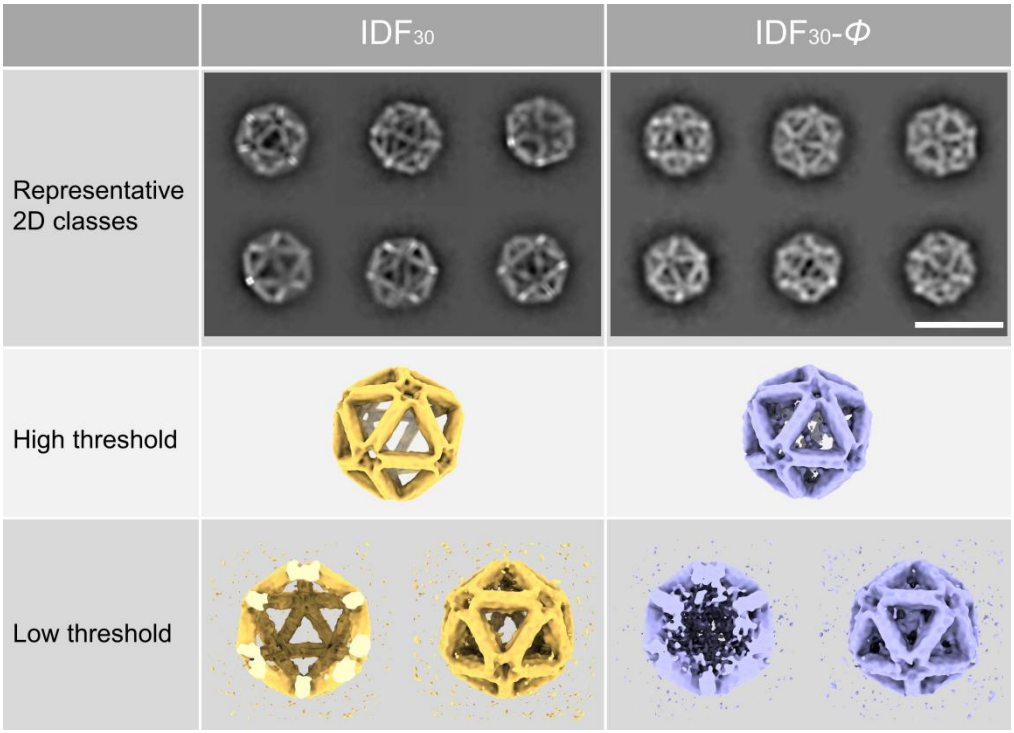

Figure S8. CryoEM image processing and analysis. Single particle analysis was applied to the data acquired from cryoEM imaging for both IDF_{30} and IDF_{30}-Φ samples. Representative images of the 2D classes and the 3D reconstructed structures at two different density threshold levels were exhibited. Scale bar: 50 nm.

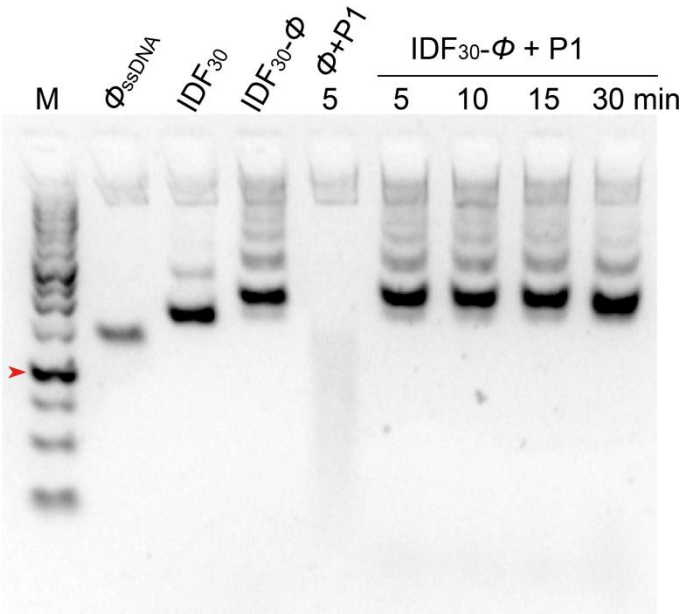

Figure S9. AGE analysis of the P1 nuclease induced ssDNA digestion for both naked and packed phiX174 genome (red arrow indicates the 1000 bp DNA marker band).

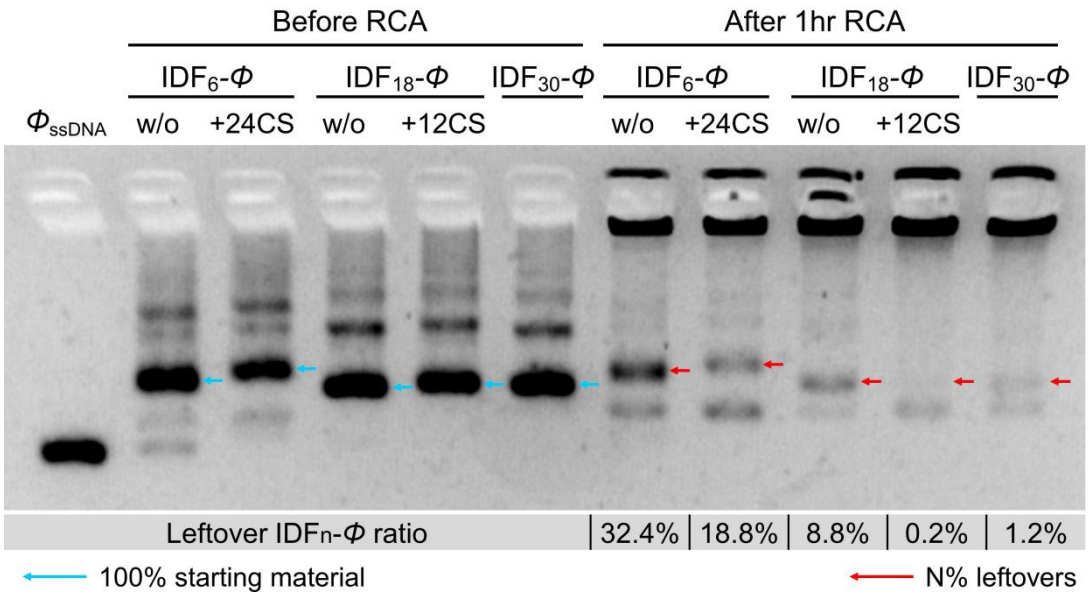

Figure S10. Anchor number dependent RCA reaction efficiency analyzed by AGE. The Φ_{ssDNA} was packed by IDF_n (n=6, 18 or 30) variants with or without the compensatory strands. The phi29 polymerase was introduced to these samples and performed the RCA reaction for 1 hour. Considering that the RCA products would gain huge molecular weight or form aggregates, the remained sharp bands with unchanged mobility (pointed by the red arrows) indicated the un-reacted complexes (a.k.a leftovers). The leftover IDF_n-Φ ratio could then be calculated by comparing the intensity of the leftover bands and the original bands (packed products without RCA reaction).

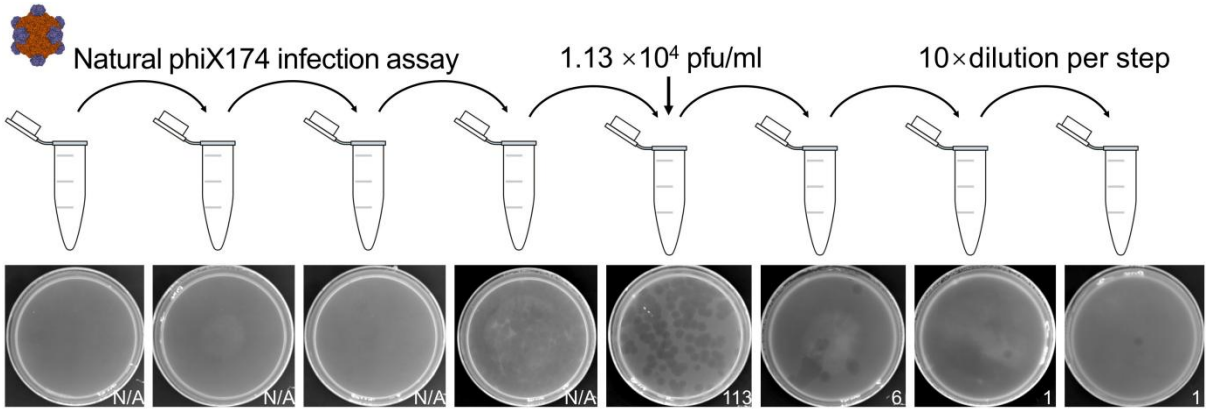

Figure S11. Natural phiX174 infection assay. As a positive control, the original solution of the phiX174 bacteriophage was applied to a sequential dilution (10× per step). 10 μL of each diluted sample was mixed with 400μL bacteria solution and incubated for 30min at 37°C (200rpm shaking), then mixed with a pre-melted 4ml 0.5% agarose medium (cooled down and maintained at 37°C) and poured onto a solid LB dish and incubated at 37°C for 2 hour.

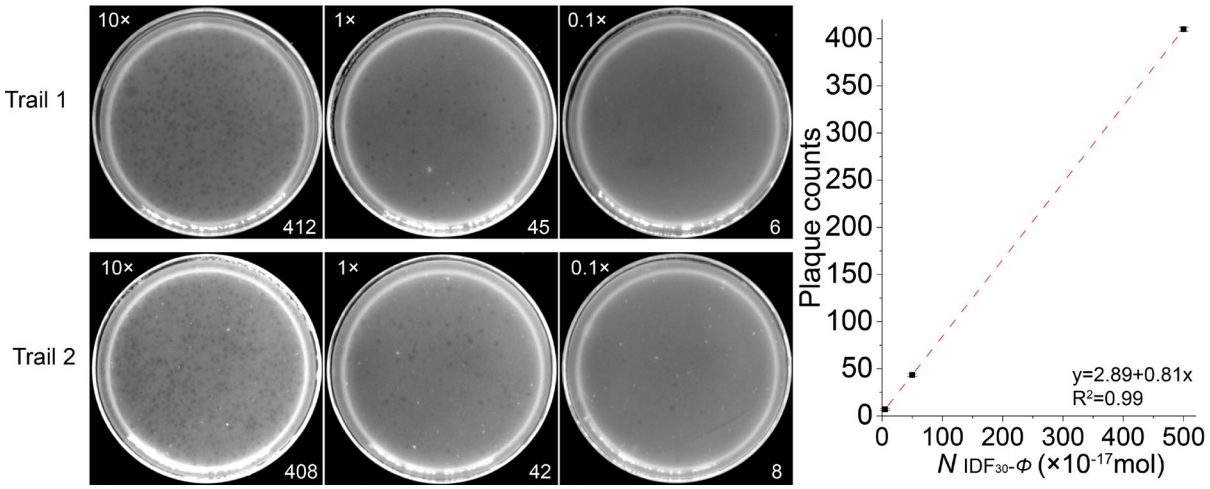

Figure S12. Concentration dependent IDF_{30}-*Φ* induced infection. Left: in two independent trails, 10, 1 and 0.1μL of 24 nM IDF_{30}-*Φ* were mixed with the 400μL E. coli solution and performed the plaque assay as described in the method section in main text. Right: the counted plaque number followed a perfect linear relationship with the added IDF_{30}-*Φ* amount. From the linear equation, a particle (IDF_{30}-*Φ*) to pfu ratio of 7.5×10^6 could be derived.

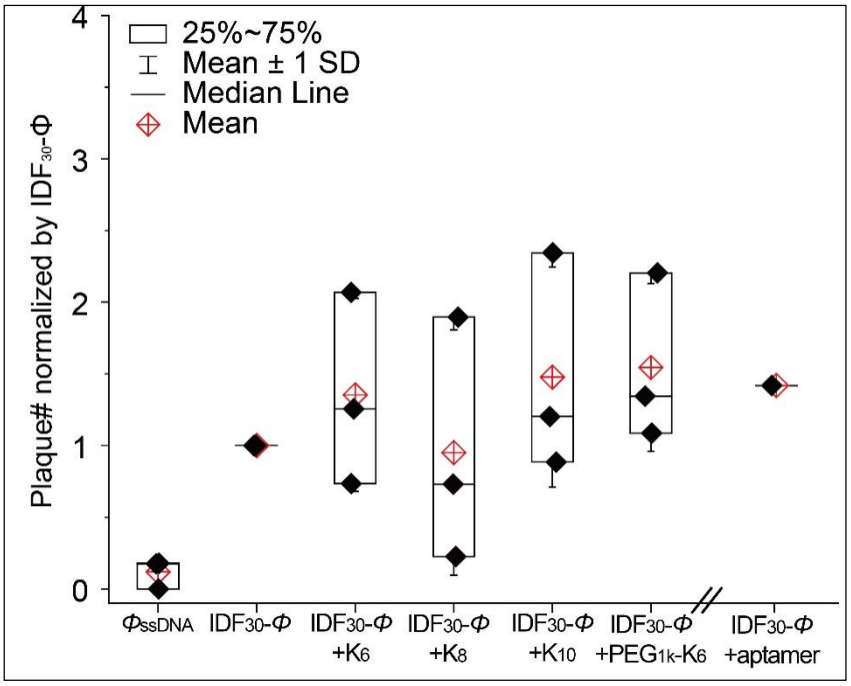

Figure S13. Infection efficiency analysis of the modified IDF_{30}-*Φ* particles. Three independent trials of K_n (n=6, 8 or 10) and PEG_{1k}-K_6 coated IDF_{30}-*Φ* were compared with the unmodified IDF_{30}-*Φ* and unpacked $Φ_{ssDNA}$. Extremely large batch to batch difference were observed, which might attribute to peptide (oligolysine) DNA disassociation at the bacterial culturing environment or peptide involved bacterial nutrition. Although K_{10} and PEG_{1k}-K_6 group yielded in average 50% more plaque formation compare to the unmodified IDF_{30}-*Φ*, it was hard to conclude that the surface charge or PEG modification played a key role in the IDF_{30}-*Φ* internalization. Meanwhile, a single test of the 30 aptamers modified IDF_{30}-*Φ* yielded a comparable number of plaques, which was not attractive enough to pursue further.

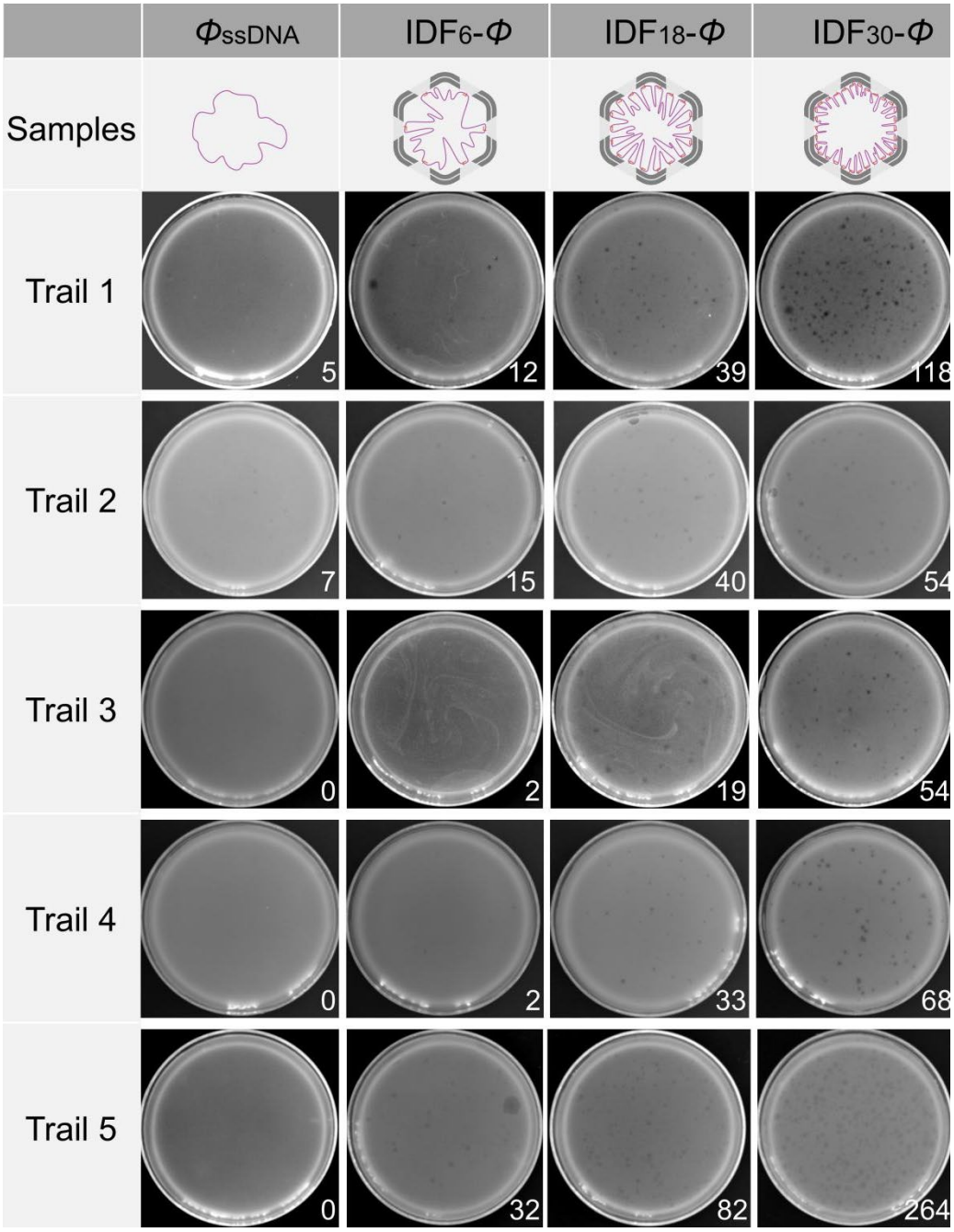

Figure S14. Five independent trials of Φ_{ssDNA} and IDF_n-Φ (n=6, 18 and 30) induced infection. Although batch to batch differences were obvious, the evidence that Φ_{ssDNA} could barely yield plaque and the trend of anchor number dependent infection efficiency were recognizable. Box analysis of the normalized data were shown in Figure 5b in the main text.

Materials

Scaffold DNA p7560 was purchased from Integrated DNA Technologies, Pte. Ltd. (USA). Single-stranded phiX174 genome was purchased from Gene Company Limited (Shanghai). DNA oligonucleotides (staple strands) were synthesized by Sangon Biotech (Shanghai) Co., Ltd. Oligolysines were synthesized by China Peptides Co., Ltd. (Shanghai). Regular chemicals and bacterial culturing materials were purchased from Corning Inc. (USA).

All of the staples participated to this study were listed in Table 1, as shown below.

Table 1. Staple strands information

Name	Sequence	Length
ico-vertex-FL-001	AGACATTTTTGTCAAATCACCGTACCCCGGTTTTTTTGATAATCAGAAA	49
ico-vertex-FL-002	AATTCTTTTTGCGTCTGGCCTAGTATCGGCCTTTTTTTCAGGAAGATCGC	49
ico-vertexF-L-003	TTTTGTTTTTTTAAAATTCGCA	22
ico-vertex-FL-004	AATTATTTTTACCGTTGTAGCGATAGGGTTGATTTTTGTGTTG	43
ico-vertex-FL-005	TAGGGTTTTTCGCTGGCAAGTGGAACGGTACGTTTTTCCAGAATCCTGA	49
ico-vertex-FL-006	TTCCACCCCCGATTTATTTTTGAGCTTGACGGG	33
ico-vertex-FL-007	ATTGCTTTTTTCCTTTTGATATAGATACATTTTTTTTCGCAAATGGTCA	49
ico-vertex-FL-008	CCAATTTTTTACTGCGGAATCATCGCGTTTTATTTTTATTCGAGCTTCA	49
ico-vertex-FL-009	TTCTATTTTTCTAATAGTAGTA	22
ico-vertex-FL-010	AGGCTTTTTTTTTGCAAAAGACCTCATATATTTTTTTTTAAAT	43
ico-vertex-FL-011	AAGTTTTTTTTGAGTAACATTAGGAATTACGATTTTTGGCATAGTAAGA	49
ico-vertex-FL-012	GCAATGCCAGGGTTTTTTTTTCCCAGTCACGAC	33
ico-vertex-FL-013	TAGACTTTTTTTTACAAACAACGCCCTGGAGTTTTTTGACTCTATGATA	49
ico-vertex-FL-014	ATAAATTTTTACAGAGGTGAGCTAAAATATCTTTTTTTTTAGGAGCACTA	49
ico-vertex-FL-015	GGCCTTTTTTTGAATCGGCTGA	22
ico-vertex-FL-016	ATGCGTTTTTCGAACTGATAGTTATCCGCTCATTTTTCAATTC	43
ico-vertex-FL-017	TCAAATTTTTCTATCGGCCTTCAGAGATAGAATTTTTCCCTTCTGACCT	49
ico-vertex-FL-018	CACACGCGTATTGGGCTTTTTGCCAGGGTGGTT	33
ico-vertex-FL-019	TCACCTTTTTGTACTCAGGAGCAGCCCTCATATTTTTGTTAGCGTAACG	49
ico-vertex-FL-020	GGGTTTTTTTTTGCTCAGTACC	22
ico-vertex-FL-021	TTTGCTTTTTTAAACAACTTTGATACCGATAGTTTTTTTGCGCCGACAA	49
ico-vertex-FL-022	CATGAGAAGTTTCCATTTTTTTTAAACGGGTAAA	33
ico-vertex-FL-023	AATAATTTTTATCCTCATTAAAACCTATTATTTTTTTCTGAAA	43
ico-vertex-FL-024	ACTAATTTTTAACACTCATCTAAAGAGGACAGTTTTTATGAACGGTGTA	49
ico-vertex-FL-025	CCGCCTTTTTGCCAGCATTGATCAACTTTAATTTTTTCATTGTGAATTA	49
ico-vertex-FL-026	TTGAGTTTTTCGCTAATATCAG	22
ico-vertex-FL-027	CATATTTTTTTCCTGATTATCCAGTACCTTTTTTTTTTACATCGGGAGAA	49
ico-vertex-FL-028	GCGCAACAGTACATAATTTTTATCAATATATGT	33
ico-vertex-FL-029	ATTTTTTTTTGCACCCAGCTAAACATAAAAACTTTTTAGGGAA	43
ico-vertex-FL-030	TCCTTTTTTTGAAAACATAGCTTTTTCAAATATTTTTTATTTTAGTTAA	49
ico-vertex-FL-031	GGCGTTTTTTTTTAGCGAACCCTTAATTGAGATTTTTATCGCCATATTT	49
ico-vertex-FL-032	TAGGATTTTTATCATTACCGCG	22
ico-vertex-FL-033	TATAATTTTTAGTACCGACAATCCTTATCATTTTTTTCCAAGAACGGGT	49
ico-vertex-FL-034	AAAAGTTTTTAAACGCAAAGAGCCATTTGGGATTTTTATTAGA	43

ico-vertex-FL-035	GCCAGTTAGCGTTTGCTTTTTCATCTTTTCATA	33
ico-vertex-FL-036	CCCTCTTTTTAGAACCGCCACAACTGGCATGATTTTTTTAAGACTCCTT	49
ico-vertex-AL-001	ACTCACATTAATTGGGCGATGGCCCGTTAATA	32
ico-vertex-AL-002	AACCGTCTATCATATCGTAAAACT	24
ico-vertex-AL-003	GATGAACGGTATCTGTTGGGAAGGAGGCCGG	31
ico-vertex-AL-004	CAGGCTGCGCAATCATCTGCCAGT	24
ico-vertex-AL-005	TCGTAACCGTGTTGCGTTGCGCTCCAAAAAT	31
ico-vertex-AL-006	ATCGGCAAAATTTTATCAACAATATCACGCA	31
ico-vertex-AL-007	GAACGCGCCTGTTGGAGGCCGATT	24
ico-vertex-AL-008	GGAGCTAAACATAATATGCAACTACGGGCGC	31
ico-vertex-AL-009	CAACATGTTTTATAGCACTAAATC	24
ico-vertex-AL-010	AGGTGCCGTAATCCCTTATAAAT	31
ico-vertex-AL-011	TTCCCAATTCTTTTGAAAATCTCCACCTTTA	24
ico-vertex-AL-012	AATTTTTTCACGTTAAGAGGAAGC	31
ico-vertex-AL-013	ATCAAAAAGATTCTAAATCGGTTGATAGCGT	32
ico-vertex-AL-014	CAGAGCATAAAGTCTACAAAGGCTAGCATCAA	24
ico-vertex-AL-015	TTTTTGAGAGATTGCGAACGAGTA	31
ico-vertex-AL-016	AGCCTTTATTTTTTGTGTCGAAATTAGCGAG	24
ico-vertex-AL-017	TCGCCTGATAAATCAACTAATGCA	31
ico-vertex-AL-018	AATACCACATTTATGCGCACGACTATTTTAA	24
ico-vertex-AL-019	GGTTGTGAATTCTTGCTGCAAGGC	23
ico-vertex-AL-020	AAAGGGGGATGTCAACGCAAGGA	31
ico-vertex-AL-021	TCCCGCCAAAATAACCTACCATATGAAGTAT	24
ico-vertex-AL-022	TGGAAGGGTTAGTCAGTTGAAAGG	31
ico-vertex-AL-023	TGGCAAATCAATGGTGCTTGTTACGCAGAAG	32
ico-vertex-AL-024	CTTAAGCTACGTTAAACGGCGGATTATATAGG	24
ico-vertex-AL-025	CTCCGTGGGAACTTAACCCCGCTT	31
ico-vertex-AL-026	TCGTAATCATGTACCTTTTTAACCGTCTTTA	24
ico-vertex-AL-027	GTCTGAGAGACTTCAGTAATAAAA	31
ico-vertex-AL-028	AGTCACACGACTCCACGCTGGTTTGAAGAAC	24
ico-vertex-AL-029	GCAGCAAGCGGTTCGGCCAACGCG	23
ico-vertex-AL-030	CATTAATGAATTGTCATAGCTGT	31
ico-vertex-AL-031	CACCAGTACAATGCACCGTAATCAAGGTGTA	31
ico-vertex-AL-032	CCATCGATAGCATGGGATCGTCACCATTAGCG	32
ico-vertex-AL-033	GGCCGCTTTTGCTTTTCGAGGTGA	24

ico-vertex-AL-034	TATCAGCTTGCTTGGTTGCTTTGAATGGGAT	31
ico-vertex-AL-035	GGGCGCGTACTATACTACAACGCC	24
ico-vertex-AL-036	GCTACAGAGGCTACAGTTAATGC	23
ico-vertex-AL-037	TGCCCGTATAATACGTAACAAAGCACAAACA	31
ico-vertex-AL-038	TTACCCAAATCATATAAGGGAACC	24
ico-vertex-AL-039	GACGGTCAATCTCAAAAATCAGGTAGAATAC	31
ico-vertex-AL-040	ATGACCATAAATTTTTGAGGACTA	24
ico-vertex-AL-041	CAGAACGAGTATGAAGCCCTTTTTACCAGAG	31
ico-vertex-AL-042	AGCTATCTTACCTCCTGAGCAAAAGAGGGTAA	32
ico-vertex-AL-043	TCATTTCAATTATGTTTAACGTCA	24
ico-vertex-AL-044	TAGATTTTCAGTCTAACGGAACAATTATCAT	31
ico-vertex-AL-045	TAATAAAACGAATGTAAATTGGGC	24
ico-vertex-AL-046	AAAAATCTAAAGTTCATTTGAATT	24
ico-vertex-AL-047	ATTTAACAATTTGAAAATAGCAG	23
ico-vertex-AL-048	ACGTCAAAAATTCCGGAATCATAAAGTTGCT	31
ico-vertex-AL-049	TAAGAATAAACATATCGCAAGACA	24
ico-vertex-AL-050	ATGCAAATCCATCATCACCTTGCTCTTAGAA	31
ico-vertex-AL-051	AATTCTTACCATAAAGGGCGACATAACGCGA	31
ico-vertex-AL-052	GCGCCAAAGACATTCAGGGATAGCATTCATCG	32
ico-vertex-AL-053	CCACCCTCATTTTAGAAACCAATC	24
ico-vertex-AL-054	TACGAGCATGTTCATTTTGACGCTAAGAGAA	31
ico-vertex-AL-055	TGGAAATACCTATGTATAAAGCCA	24
ico-vertex-AL-056	GCGCGTTTTCATGGTGAATTATC	23
ico-vertex-AL-057	GCTTTTGATGATTTCGGCATTTTC	24
ico-vertex-AL-058	AAACCGAGGAATACAGGAGTGTACGCCGCCA	31
ico-vertex-AL-059	CCAGTTACAAAATACGCAATAATA	24
ico-vertex-AL-060	TATTCATTAAATTAAACAGCCATAAACATAT	31
ico-FL-S1-001	TATTTAAAAAACAGGAACGTCAAAGGGCGAAA	32
ico-FL-S1-002	GCGAGCTGTTTAGCTACCGGAGAGGGTAGCTA	32
ico-FL-S1-003	TTCAAAAGCAGCTTTCAGCGCCATTCGCCATT	32
ico-FL-S1-004	TCGTCGGTGCGGCCCTAACAACCCGTCGGATT	32
ico-FL-S1-005	CCAATAGGTTGTTAAACCTAATGAGTGAGCTA	32
ico-FL-S1-006	AAGAAAGCGCGAACGTATATAATGCTGTAGCT	32
ico-FL-S1-007	AAAATGTTATCCAATATTAAGCAATAAAGCCT	32
ico-FL-S1-008	TGCCCGAAACGACGGCGGATGTTCTTCTAAGT	32

ico-FL-S1-009	ACCGAACGACATAAATTAATGAGTAAACAGGG	32
ico-FL-S1-010	ATCACTTGCACCAGTGTGGCCCTGAGAGAGTT	32
ico-FL-S1-011	TAAAAGAGTTTATAATATGTTCAGCTAATGCA	32
ico-FL-S1-012	TAAATGAATTTTGTCGTTAATGCGCCGCTACA	32
ico-FL-S1-013	GTCAGGATCAGACCGGAGGAATTGCGAATAAT	32
ico-FL-S1-014	AAACGAAATGCCACTAAGTTCAGAAAACGAGA	32
ico-FL-S1-015	ACGATAAAATCATAACACGGAGATTTGTATCA	32
ico-FL-S1-016	ACCAGAAGGATTTTAAGAAGAAAAATCTACGT	32
ico-FL-S1-017	TACATTTGTAGATTAGTTATACTTCTGAATAA	32
ico-FL-S1-018	TATTAATTAACCTTGCGAGCCAGCAGCAAATG	32
ico-FL-S1-019	TTTTGAATAAGAATACTTTATCAAAATCATAG	32
ico-FL-S1-020	TTTTCGAGCAACATGTACAGGAAAAACGCTCA	32
ico-FL-S1-021	GCAAGCCGAAGTACCGGCCACCCTCAGAGCCA	32
ico-FL-S1-022	CAAGAGAAACCATCGCCTTGCAGGGAGTTAAA	32
ico-FL-S1-023	ATTGGCCTGCGCATAGAAGAACCGGATATTCA	32
ico-FL-S1-024	CCCTGAACGGATTCGCCGCAGAGGCGAATTAT	32
ico-FL-S1-025	GCCTTAAATCTGACCTTAAATAAGGCGTTAAA	32
ico-FL-S1-026	AAGTATAGAAGTGCCGAACGTCACCAATGAAA	32
ico-FL-S1-027	AACCGCCTCACCGGAAGTAAGCGTCATACATG	32
ico-FL-S1-028	CGCCACCACCCACAAGACAATGAAATAGCAAT	32
ico-FL-S1-029	CATACATAGTATGTTATCCAGAGCCTAATTTG	32
ico-FL-S1-030	TATCCGGTCAAGCAAATTCATATGGTTTACCA	32
ico-AL-S1-001	CCCAAATCGGACTCCAAGATTGTACACTATTAAAAGGGAGGTTTGGAATG GGGTCG	56
ico-AL-S1-002	GAGTCTGGAATTAATGTATTTTCAACCGTTCTAATCATATATCAATATAGAG AATC	56
ico-AL-S1-003	TCTTCGCTCCAGGCAACGGCACCGCTTCTGGTTGGGTAACGCCTGAGTA GCTGGCG	56
ico-AL-S1-004	GTCACGTTGAGCGAGTGCCATCTGCATCAACAACGACGACTCCTGTAGTG GGCGCA	56
ico-AL-S1-005	TCGGGAAACTGGGGTGTCAGCTCAGCATAAAGGGCGGTTTAACATACGG CCAGCTG	56
ico-AL-S1-006	AGTTTCATATTGCTGAGGCGAGAAGATGGCTTTTGACCATAGAGGTCAAC AGTTGA	56
ico-AL-S1-007	ACCCTGTATAGCAAAAAATCATACAGGCAAGGTTTAGAACAGTTTTGCGC GGGAGA	56
ico-AL-S1-008	TGAATTGTGCCAGGGTCAGTGCCAAGCTTTCTTTTACGCTTTCGACAATGA CAATG	56

ico-AL-S1-009	GATCCCCGGGTTGGTGCATTTCTCCGAACTCTTGAAATTGCCCTAAAAGC TCGAAT	56
ico-AL-S1-010	ATCCTGTTTCACCGCCAGACGGGCAACAGCTGTAGCCCGAAATACTTCGT TCCGAA	56
ico-AL-S1-011	GAAAAATATAAACAACCAGTGAGGGTCCAGACGCTGTCTTAAGGTAAATC CTAATT	56
ico-AL-S1-012	GCTTTCCTCGCCGCGCTCTTTCCAGCGTAACCTTTAGACAGTAGCGGTTC AGAGCG	56
ico-AL-S1-013	AAGGAGCCACAACTAAAAGCAAACGTGAGAATAACAGCTTCAACAGTTTA TCGGTT	56
ico-AL-S1-014	ATAGTCAGCTTTAAACCGAAGGCAGAATCCCCCTTCAAATGTCATAAACG GATTGC	56
ico-AL-S1-015	GTTACTTAAAAGTACACCTCGTTTATACCAAGCAACTTTGTTGACCCCGAG GCGCA	56
ico-AL-S1-016	AAGATTCAGACGTTGGGAACTGGCTCATTATAACGCCAAAATCATTTTGAT TTAGG	56
ico-AL-S1-017	TAAAACAGTGTTTGGAAGCCGTCATCAATATATACAGTAAAGATGATGAAA TTGCG	56
ico-AL-S1-018	ACCCTCAACACGCTGATTCTGTAACCGCCTGCAAGGTTATGCGGTCAGTG GTCAGT	56
ico-AL-S1-019	TTATATAAATAGTGAAGTGGCACAACGCTGAGGAGAAAACGATAGCTTAA ATGCTG	56
ico-AL-S1-020	ATTATTTACCATTGCAAATTTAGGACAATATTCTGGCCAAGCTGGTAAGAT TCACC	56
ico-AL-S1-021	ATGTACCGTCAGAACCCACTCATCCTCAGAACTCCACAGAGTTTAGTAAG TTTCGT	56
ico-AL-S1-022	AGCATCGGCGCTGAGGCCACGCATAACCGATATTCATGAGAAGTATTATA GCAACG	56
ico-AL-S1-023	AAGGCTTGATCTTGACGCTGGCTGACCTTCATGTTTAATTCAGGAGGTAG AAACAC	56
ico-AL-S1-024	CATCAAGACAAAATCGCTGATTGCTTTGAATATAATGGAATTAGACGGTTA ATTAC	56
ico-AL-S1-025	GTTTAGTACCGTGTGAAAATTTAATGGTTTGACAGTAGGGTCCCGACTGTT ATACA	56
ico-AL-S1-026	GTTTGCCTAGGCCGGATCGAGAGGACCATTACCCCCCTTACAAAATCAAG ACTGTA	56
ico-AL-S1-027	CGGGGTCACCGTTCCACCAGAGCCGCAGTCTCTATTTCGGAGCCAGAAA GTAACAG	56
ico-AL-S1-028	TAGCCGAAAGCAAGAAAATTGAGTTAAGCCCACCCAAAAGCCTCAGAGCC AGAAGG	56
ico-AL-S1-029	AAATAAGAAGCGTCTTGCAAACGTCTTACCAAGAGAGAATCAATTTTATTT GTTTA	56
ico-AL-S1-030	GGGAAGGTATAGAAAATCAGATATTATTTTGTCGACTTGACACCACGGAC GGAAAT	56

ico-AL-S2-001	AGCCCCAATTGTAAACACTACGTGAACCATCA	32
ico-AL-S2-002	ATAACCTGAAAAGGTGTCAGGTCATTGCCTGA	32
ico-AL-S2-003	ACTCCAGCGGTGAGAAGCGATCGGTGCGGGCC	32
ico-AL-S2-004	CCGACAGTGGGCACGAGACCGTAATGGGATAG	32
ico-AL-S2-005	TTAAATTTAACGCCATACTGCCCGCTTTCCAG	32
ico-AL-S2-006	GAAAGCCGGAAAGGAGAAGTACGGTGTCTGGA	32
ico-AL-S2-007	GCATTAACTAGACTGGTACCAAAAACATTATG	32
ico-AL-S2-008	GTTGTAAACGTTATTATAAGTGTCCTTAGTGC	32
ico-AL-S2-009	CGCATTTCAACCACCACTCGATAAAGACGGAG	32
ico-AL-S2-010	TTTCTTTTCCTGAGTAGCCCCAGCAGGCGAAA	32
ico-AL-S2-011	GAAGTGTTTCTGTCCAGATAAGTCCTGAACAA	32
ico-AL-S2-012	ATCTAAAGTTTTCTGTCGAGCACGTATAACGT	32
ico-AL-S2-013	AAGCGAACTAGAGAGTAAAAAAAAGGCTCCAA	32
ico-AL-S2-014	ATACGTAAGAGGCAAACTTTACCCTGACTATT	32
ico-AL-S2-015	GCAACACTAACCAAAACCGCGACCTGCTCCAT	32
ico-AL-S2-016	CCTTATGCGAGCGGAACATTATTACAGGTAGA	32
ico-AL-S2-017	ACAACTAAAGGATTTACAAAATTATTTGCACG	32
ico-AL-S2-018	GAGTGAATAATTTTCCGAACCTCAAATATCAA	32
ico-AL-S2-019	GAAAGCGTGGCTATTATCCGGCTTAGGTTGGG	32
ico-AL-S2-020	AACAACGCCCAGTAATCAATCGTCTGAAATGG	32
ico-AL-S2-021	ATTAAACCTTTTTATTAGCCCAATAGGAACCC	32
ico-AL-S2-022	TGACAACAGGATTAGGCTCAGCAGCGAAAGAC	32
ico-AL-S2-023	CAGACCAGTGATATTCTGCTCATTCAGTGAAT	32
ico-AL-S2-024	ACAATAACAAAGTCAGAAGATGATGAAACAAA	32
ico-AL-S2-025	TTTCATCTTCAAGATTTTACTAGAAAAAGCCT	32
ico-AL-S2-026	AGGCGGATCCCGGAATGTAGCGACAGAATCAA	32
ico-AL-S2-027	ATCAAAATCCCTCAGATGGTAATAAGTTTTAA	32
ico-AL-S2-028	AGAGATAAGAACCACCAAGAAAAGTAAGCAGA	32
ico-AL-S2-029	ATTACGCAAAGGTGGCTTATTTATCCCAATCC	32
ico-AL-S2-030	CCCAATAGATTCTAAGTCAACCGATTGAGGGA	32
ico-FL-S2-001	GGAACCCTAAGAACGTAAGTTTTTCAAGAGTCTAAGCAAA	40
ico-FL-S2-002	AGCATGTCAGCTGATAAGCAAACAGATATTCATTTGGGGC	40
ico-FL-S2-003	GATTAAGTGCCGGAAAATTACGCCAATGTGTAGGTAAAGA	40
ico-FL-S2-004	TTGAGGGGTTAAATGTGGTGTAGACCAGCTTTTAAGCAAC	40
ico-FL-S2-005	CGGGGAGATGTAAAGCCCTGTCGTAGCCGGAATTTTTTAA	40

ico-FL-S2-006	GATTTAGTAGAGCTTATCCATATATTTTTGCGAGGAAGGG	40
ico-FL-S2-007	TAAAAATTCAAAGAATATACTTTTCAGAGGGGGTAATAGT	40
ico-FL-S2-008	CTAATCTACAGGAGAACAACCTTACTCGTATTAAATCCTT	40
ico-FL-S2-009	TTCCTGTGGACCTCCTGGTACCGACATCGCCATTAAAAAT	40
ico-FL-S2-010	CAAAAGAAATTGCCCTTGATGGTGTTTGATTAGTAATAAC	40
ico-FL-S2-011	AATAATCGGACGACAAATATCCCAGTAATTCTCCACCGAG	40
ico-FL-S2-012	AAAGGGATACCACACCCGTTAGAACACGCTGCGACGTTAG	40
ico-FL-S2-013	ATTTCTTAAGAAAGGATTTAATTGTCAGCGGATCCAACAG	40
ico-FL-S2-014	CCGAAAGACTCAAATGAAGCAAAGTATTCATTCCAACCTA	40
ico-FL-S2-015	GAACTGACCGCGAAACGCCGGAACCAGCGATTACCAGACG	40
ico-FL-S2-016	GATACATACCAGTCAGTCAGTTGAGCGGAACAAAGAAACC	40
ico-FL-S2-017	GATGAATAATCCTGATAAATAAAGGCAATTCAATAGATAA	40
ico-FL-S2-018	AATTGAGGAACAGTGCTCAATATCTATTAACAATCGTCGC	40
ico-FL-S2-019	AAGAACGCAAGAGTCACTATATGTAGATTAAGGACAATAT	40
ico-FL-S2-020	GGGACATTACCGCCAGCATTGGCATATCCAGACAGAGGCA	40
ico-FL-S2-021	TGTAGCATCGCCACCCTAACACTGCCGCCACCGAGAACAA	40
ico-FL-S2-022	AAGACTTTTATTCGGTAACGAGGGAGAGGCTGAGACTCCT	40
ico-FL-S2-023	TTGAGATGCAAGAGTACCCTGACGTGAGGCAGGTCAGACG	40
ico-FL-S2-024	ACCTTTTTCCAAGTTAAAACAAAAGAGAATTAACTGAACA	40
ico-FL-S2-025	ACGCTCAAAATACCGATCATATGCTGCGGGAGGTTTTGAA	40
ico-FL-S2-026	GGTCATAGCATTAGCATTAGCGTCCCAGTAGCGTTGATAT	40
ico-FL-S2-027	CCCCTGCCTGAATTTAGTGCCTTGTGGAAAGCACCACCGG	40
ico-FL-S2-028	ACGGAATAATAATAAGCAAAGTTACCACCACCCTCAGAGC	40
ico-FL-S2-029	CCTTTACACGCTAACGAACGATTTTCCTGAATAGAAAATA	40
ico-FL-S2-030	ACCGTCACCACAATCAAAATATTGAATAAGTTAGAAGGCT	40
ico-AL-S2-anchor-10-001	TTAGCCCCAATTGTAAACACTACGTGAACCATCAAGTACCTCGC	44
ico-AL-S2-anchor-10-002	TTATAACCTGAAAAGGTGTCAGGTCATTGCCTGAGAAAGGTCGC	44
ico-AL-S2-anchor-10-003	TTACTCCAGCGGTGAGAAGCGATCGGTGCGGGCCGTTGAACAGC	44
ico-AL-S2-anchor-10-004	TTCCGACAGTGGGCACGAGACCGTAATGGGATAGCAGCGACGAG	44
ico-AL-S2-anchor-10-005	TTTTAAATTTAACGCCATACTGCCCGCTTTCCAGGGACGCTCGA	44
ico-AL-S2-anchor-10-006	TTGAAAGCCGGAAAGGAGAAGTACGGTGTCTGGAGATAAAACTC	44

ico-AL-S2-anchor-10-007	TTGCATTAACTAGACTGGTACCAAAAACATTATGTAATAACCTG	44
ico-AL-S2-anchor-10-008	TTGTTGTAAACGTTATTATAAGTGTCCTTAGTGCACCCCTCAGC	44
ico-AL-S2-anchor-10-009	TTCGCATTTCAACCACCACTCGATAAAGACGGAGTTTATAGGTC	44
ico-AL-S2-anchor-10-010	TTTTTCTTTTCCTGAGTAGCCCCAGCAGGCGAAAGGTAATAAGA	44
ico-AL-S2-anchor-10-011	TTGAAGTGTTTCTGTCCAGATAAGTCCTGAACAAAACACCATCC	44
ico-AL-S2-anchor-10-012	TTATCTAAAGTTTTCTGTCGAGCACGTATAACGTGCAAGGTCCA	44
ico-AL-S2-anchor-10-013	TTAAGCGAACTAGAGAGTAAAAAAAAGGCTCCAAGGCGTCGCGT	44
ico-AL-S2-anchor-10-014	TTATACGTAAGAGGCAAACTTTACCCTGACTATTATGCCTACAG	44
ico-AL-S2-anchor-10-015	TTGCAACACTAACCAAAACCGCGACCTGCTCCATCAGTCGGGAG	44
ico-AL-S2-anchor-10-016	TTCCTTATGCGAGCGGAACATTATTACAGGTAGATATCAAAATA	44
ico-AL-S2-anchor-10-017	TTACAACTAAAGGATTTACAAAATTATTTGCACGATCATGGTGG	44
ico-AL-S2-anchor-10-018	TTGAGTGAATAATTTTCCGAACCTCAAATATCAAAGAAATTTCA	44
ico-AL-S2-anchor-10-019	TTGAAAGCGTGGCTATTATCCGGCTTAGGTTGGGATCACGTTCT	44
ico-AL-S2-anchor-10-020	TTAACAACGCCCAGTAATCAATCGTCTGAAATGGATTAGGGTTA	44
ico-AL-S2-anchor-10-021	TTATTAAACCTTTTTATTAGCCCAATAGGAACCCTTTTGCAAGC	44
ico-AL-S2-anchor-10-022	TTTGACAACAGGATTAGGCTCAGCAGCGAAAGACCCACCAAGTC	44
ico-AL-S2-anchor-10-023	TTCAGACCAGTGATATTCTGCTCATTCAGTGAATTCGGAAACCT	44
ico-AL-S2-anchor-10-024	TTACAATAACAAAGTCAGAAGATGATGAAACAAACCAAGATTTG	44
ico-AL-S2-anchor-10-025	TTTTTCATCTTCAAGATTTTACTAGAAAAAGCCTCGGTGGTCTA	44
ico-AL-S2-anchor-10-026	TTAGGCGGATCCCGGAATGTAGCGACAGAATCAACGACCCTCGG	44
ico-AL-S2-anchor-10-027	TTATCAAAATCCCTCAGATGGTAATAAGTTTTAATCGGCAATCT	44
ico-AL-S2-anchor-10-028	TTAGAGATAAGAACCACCAAGAAAAGTAAGCAGAACGACATTAG	44

ico-AL-S2-anchor-10-029	TTATTACGCAAAGGTGGCTTATTTATCCCAATCCATCTCTTCCA	44
ico-AL-S2-anchor-10-030	TTCCCAATAGATTCTAAGTCAACCGATTGAGGGACTACGCGATT	44
ico-AL-S2-anchor-20-001	TTAGCCCCAATTGTAAACACTACGTGAACCATCAGCTTGCCTTTAGTACCTCGC	54
ico-AL-S2-anchor-20-002	TTATAACCTGAAAAGGTGTCAGGTCATTGCCTGAAGTTGATGGCGAAAGGTCGC	54
ico-AL-S2-anchor-20-003	TTACTCCAGCGGTGAGAAGCGATCGGTGCGGGCCCCTATTAGTGGTTGAACAGC	54
ico-AL-S2-anchor-20-004	TTCCGACAGTGGGCACGAGACCGTAATGGGATAGAGCCTCAACGCAGCGACGAG	54
ico-AL-S2-anchor-20-005	TTTTAAATTTAACGCCATACTGCCCGCTTTCCAGGGCTTTAACCGGACGCTCGA	54
ico-AL-S2-anchor-20-006	TTGAAAGCCGGAAAGGAGAAGTACGGTGTCTGGATCATGGAAGCGATAAAACTC	54
ico-AL-S2-anchor-20-007	TTGCATTAACTAGACTGGTACCAAAAACATTATGATAATCTCTTTAATAACCTG	54
ico-AL-S2-anchor-20-008	TTGTTGTAAACGTTATTATAAGTGTCCTTAGTGCCGCTTGGTCAACCCCTCAGC	54
ico-AL-S2-anchor-20-009	TTCGCATTTCAACCACCACTCGATAAAGACGGAGGCACAGAATGTTTATAGGTC	54
ico-AL-S2-anchor-20-010	TTTTTCTTTTCCTGAGTAGCCCCAGCAGGCGAAATAGTTGAAATGGTAATAAGA	54
ico-AL-S2-anchor-20-011	TTGAAGTGTTTCTGTCCAGATAAGTCCTGAACAAGAGTGGCATTAACACCATCC	54
ico-AL-S2-anchor-20-012	TTATCTAAAGTTTTCTGTCGAGCACGTATAACGTACCTTTAGCAGCAAGGTCCA	54
ico-AL-S2-anchor-20-013	TTAAGCGAACTAGAGAGTAAAAAAAAGGCTCCAACTGGTTGAACGGCGTCGCGT	54
ico-AL-S2-anchor-20-014	TTATACGTAAGAGGCAAACTTTACCCTGACTATTAGCATCACCCATGCCTACAG	54
ico-AL-S2-anchor-20-015	TTGCAACACTAACCAAAACCGCGACCTGCTCCATACATCATAGGCAGTCGGGAG	54
ico-AL-S2-anchor-20-016	TTCCTTATGCGAGCGGAACATTATTACAGGTAGAACCGTCAAACTATCAAAATA	54
ico-AL-S2-anchor-20-017	TTACAACTAAAGGATTTACAAAATTATTTGCACGACTGGTCATAATCATGGTGG	54
ico-AL-S2-anchor-20-018	TTGAGTGAATAATTTTCCGAACCTCAAATATCAACATCCTTCATAGAAATTTCA	54
ico-AL-S2-anchor-20-019	TTGAAAGCGTGGCTATTATCCGGCTTAGGTTGGGGCATGAAGTAATCACGTTCT	54
ico-AL-S2-anchor-20-020	TTAACAACGCCCAGTAATCAATCGTCTGAAATGGGATTAAGCTCATTAGGGTTA	54

ico-AL-S2-anchor-20-021	TTATTAAACCTTTTTATTAGCCCAATAGGAACCCAGGCCACGTATTTTGCAAGC	54
ico-AL-S2-anchor-20-022	TTTGACAACAGGATTAGGCTCAGCAGCGAAAGACGGCAGACTTGCCACCAAGTC	54
ico-AL-S2-anchor-20-023	TTCAGACCAGTGATATTCTGCTCATTCAGTGAATGCGCATAATCTCGGAAACCT	54
ico-AL-S2-anchor-20-024	TTACAATAACAAAGTCAGAAGATGATGAAACAAAAAAAAAGCCTCCAAGATTTG	54
ico-AL-S2-anchor-20-025	TTTTTCATCTTCAAGATTTTACTAGAAAAAGCCTCCCTTCGGGGCGGTGGTCTA	54
ico-AL-S2-anchor-20-026	TTAGGCGGATCCCGGAATGTAGCGACAGAATCAAATTAGCCTTGCGACCCTCGG	54
ico-AL-S2-anchor-20-027	TTATCAAAATCCCTCAGATGGTAATAAGTTTTAAATTTTGCATCTCGGCAATCT	54
ico-AL-S2-anchor-20-028	TTAGAGATAAGAACCACCAAGAAAAGTAAGCAGAAGCATCAGTGACGACATTAG	54
ico-AL-S2-anchor-20-029	TTATTACGCAAAGGTGGCTTATTTATCCCAATCCAAAAGACAGAATCTCTTCCA	54
ico-AL-S2-anchor-20-030	TTCCCAATAGATTCTAAGTCAACCGATTGAGGGAAGCAAAGCCTCTACGCGATT	54
ico-AL-S2-anchor-30-001	TTAGCCCCAATTGTAAACACTACGTGAACCATCAGCGCCTTTACGCTTGCCTTTAGTACCTCGC	64
ico-AL-S2-anchor-30-002	TTATAACCTGAAAAGGTGTCAGGTCATTGCCTGACAGAATCGTTAGTTGATGGCGAAAGGTCGC	64
ico-AL-S2-anchor-30-003	TTACTCCAGCGGTGAGAAGCGATCGGTGCGGGCCTGATTTCTTACCTATTAGTGGTTGAACAGC	64
ico-AL-S2-anchor-30-004	TTCCGACAGTGGGCACGAGACCGTAATGGGATAGCATAAACGCAAGCCTCAACGCAGCGACGAG	64
ico-AL-S2-anchor-30-005	TTTTAAATTTAACGCCATACTGCCCGCTTTCCAGACAATTCAGCGGCTTTAACCGGACGCTCGA	64
ico-AL-S2-anchor-30-006	TTGAAAGCCGGAAAGGAGAAGTACGGTGTCTGGAAACTTCTGCGTCATGGAAGCGATAAAACTC	64
ico-AL-S2-anchor-30-007	TTGCATTAACTAGACTGGTACCAAAAACATTATGCTGGAGACAAATAATCTCTTTAATAACCTG	64
ico-AL-S2-anchor-30-008	TTGTTGTAAACGTTATTATAAGTGTCCTTAGTGCTACCGCGCTTCGCTTGGTCAACCCCTCAGC	64
ico-AL-S2-anchor-30-009	TTCGCATTTCAACCACCACTCGATAAAGACGGAGAAGAAACGCGGCACAGAATGTTTATAGGTC	64
ico-AL-S2-anchor-30-010	TTTTTCTTTTCCTGAGTAGCCCCAGCAGGCGAAAATAACCGGAGTAGTTGAAATGGTAATAAGA	64
ico-AL-S2-anchor-30-011	TTGAAGTGTTTCTGTCCAGATAAGTCCTGAACAAGTCGGGAGAGGAGTGGCATTAACACCATCC	64
ico-AL-S2-anchor-30-012	TTATCTAAAGTTTTCTGTCGAGCACGTATAACGTTAGCTCCTAGACCTTTAGCAGCAAGGTCCA	64

ico-AL-S2-anchor-30-013	TTAAGCGAACTAGAGAGTAAAAAAAAGGCTCCAAGCTTCAATATCTGGTTGAACGGCGTCGCGT	64
ico-AL-S2-anchor-30-014	TTATACGTAAGAGGCAAACTTTACCCTGACTATTATTTAATACCAGCATCACCCATGCCTACAG	64
ico-AL-S2-anchor-30-015	TTGCAACACTAACCAAAACCGCGACCTGCTCCATCAAAGGATAAACATCATAGGCAGTCGGGAG	64
ico-AL-S2-anchor-30-016	TTCCTTATGCGAGCGGAACATTATTACAGGTAGAACCAGCATTAACCGTCAAACTATCAAAATA	64
ico-AL-S2-anchor-30-017	TTACAACTAAAGGATTTACAAAATTATTTGCACGGACTGGAAACACTGGTCATAATCATGGTGG	64
ico-AL-S2-anchor-30-018	TTGAGTGAATAATTTTCCGAACCTCAAATATCAAGAACGGAAAACATCCTTCATAGAAATTTCA	64
ico-AL-S2-anchor-30-019	TTGAAAGCGTGGCTATTATCCGGCTTAGGTTGGGTGGTAACGCTGCATGAAGTAATCACGTTCT	64
ico-AL-S2-anchor-30-020	TTAACAACGCCCAGTAATCAATCGTCTGAAATGGGCATCATCTTGATTAAGCTCATTAGGGTTA	64
ico-AL-S2-anchor-30-021	TTATTAAACCTTTTTATTAGCCCAATAGGAACCCTGTAACCATAAGGCCACGTATTTTGCAAGC	64
ico-AL-S2-anchor-30-022	TTTGACAACAGGATTAGGCTCAGCAGCGAAAGACCTTTATCAGCGGCAGACTTGCCACCAAGTC	64
ico-AL-S2-anchor-30-023	TTCAGACCAGTGATATTCTGCTCATTCAGTGAATTAAGCATTTGGCGCATAATCTCGGAAACCT	64
ico-AL-S2-anchor-30-024	TTACAATAACAAAGTCAGAAGATGATGAAACAAAAACGAACCATAAAAAAGCCTCCAAGATTTG	64
ico-AL-S2-anchor-30-025	TTTTTCATCTTCAAGATTTTACTAGAAAAAGCCTATTTTTCGTCCCCTTCGGGGCGGTGGTCTA	64
ico-AL-S2-anchor-30-026	TTAGGCGGATCCCGGAATGTAGCGACAGAATCAACGTGTGAATCATTAGCCTTGCGACCCTCGG	64
ico-AL-S2-anchor-30-027	TTATCAAAATCCCTCAGATGGTAATAAGTTTTAATTTGAGTCTCATTTTGCATCTCGGCAATCT	64
ico-AL-S2-anchor-30-028	TTAGAGATAAGAACCACCAAGAAAAGTAAGCAGACACCAGAAGCAGCATCAGTGACGACATTAG	64
ico-AL-S2-anchor-30-029	TTATTACGCAAAGGTGGCTTATTTATCCCAATCCCCTGCATACGAAAAGACAGAATCTCTTCCA	64
ico-AL-S2-anchor-30-030	TTCCCAATAGATTCTAAGTCAACCGATTGAGGGAAACGCTGAATAGCAAAGCCTCTACGCGATT	64
ico-FL-S2-aptamer-anchor-001	GGAACCCTAAGAACGTAAGTTTTTCAAGAGTCTAAGCAAATTTGAGAGTTAGGAATGT	58
ico-FL-S2-aptamer-anchor-002	AGCATGTCAGCTGATAAGCAAACAGATATTCATTTGGGGCTTTGAGAGTTAGGAATGT	58
ico-FL-S2-aptamer-anchor-003	GATTAAGTGCCGGAAAATTACGCCAATGTGTAGGTAAAGATTTGAGAGTTAGGAATGT	58

ico-FL-S2-aptamer-anchor-004	TTGAGGGGTTAAATGTGGTGTAGACCAGCTTTTAAGCAACTTTGAGAGTTAGGAATGT	58
ico-FL-S2-aptamer-anchor-005	CGGGGAGATGTAAAGCCCTGTCGTAGCCGGAATTTTTTAATTTGAGAGTTAGGAATGT	58
ico-FL-S2-aptamer-anchor-006	GATTTAGTAGAGCTTATCCATATATTTTTGCGAGGAAGGGTTTGAGAGTTAGGAATGT	58
ico-FL-S2-aptamer-anchor-007	TAAAAATTCAAAGAATATACTTTTCAGAGGGGGTAATAGTTTTGAGAGTTAGGAATGT	58
ico-FL-S2-aptamer-anchor-008	CTAATCTACAGGAGAACAACCTTACTCGTATTAAATCCTTTTTGAGAGTTAGGAATGT	58
ico-FL-S2-aptamer-anchor-009	TTCCTGTGGACCTCCTGGTACCGACATCGCCATTAAAAATTTTGAGAGTTAGGAATGT	58
ico-FL-S2-aptamer-anchor-010	CAAAAGAAATTGCCCTTGATGGTGTTTGATTAGTAATAACTTTGAGAGTTAGGAATGT	58
ico-FL-S2-aptamer-anchor-011	AATAATCGGACGACAAATATCCCAGTAATTCTCCACCGAGTTTGAGAGTTAGGAATGT	58
ico-FL-S2-aptamer-anchor-012	AAAGGGATACCACACCCGTTAGAACACGCTGCGACGTTAGTTTGAGAGTTAGGAATGT	58
ico-FL-S2-aptamer-anchor-013	ATTTCTTAAGAAAGGATTTAATTGTCAGCGGATCCAACAGTTTGAGAGTTAGGAATGT	58
ico-FL-S2-aptamer-anchor-014	CCGAAAGACTCAAATGAAGCAAAGTATTCATTCCAACCTATTTGAGAGTTAGGAATGT	58
ico-FL-S2-aptamer-anchor-015	GAACTGACCGCGAAACGCCGGAACCAGCGATTACCAGACGTTTGAGAGTTAGGAATGT	58
ico-FL-S2-aptamer-anchor-016	GATACATACCAGTCAGTCAGTTGAGCGGAACAAAGAAACCTTTGAGAGTTAGGAATGT	58
ico-FL-S2-aptamer-anchor-017	GATGAATAATCCTGATAAATAAAGGCAATTCAATAGATAATTTGAGAGTTAGGAATGT	58
ico-FL-S2-aptamer-anchor-018	AATTGAGGAACAGTGCTCAATATCTATTAACAATCGTCGCTTTGAGAGTTAGGAATGT	58
ico-FL-S2-aptamer-anchor-019	AAGAACGCAAGAGTCACTATATGTAGATTAAGGACAATATTTTGAGAGTTAGGAATGT	58

ico-FL-S2-aptamer-anchor-020	GGGACATTACCGCCAGCATTGGCATATCCAGACAGAGGCATTTGAGAGTTAGGAATGT	58
ico-FL-S2-aptamer-anchor-021	TGTAGCATCGCCACCCTAACACTGCCGCCACCGAGAACAATTTGAGAGTTAGGAATGT	58
ico-FL-S2-aptamer-anchor-022	AAGACTTTTATTCGGTAACGAGGGAGAGGCTGAGACTCCTTTTGAGAGTTAGGAATGT	58
ico-FL-S2-aptamer-anchor-023	TTGAGATGCAAGAGTACCCTGACGTGAGGCAGGTCAGACGTTTGAGAGTTAGGAATGT	58
ico-FL-S2-aptamer-anchor-024	ACCTTTTTCCAAGTTAAAACAAAAGAGAATTAACTGAACATTTGAGAGTTAGGAATGT	58
ico-FL-S2-aptamer-anchor-025	ACGCTCAAAATACCGATCATATGCTGCGGGAGGTTTTGAATTTGAGAGTTAGGAATGT	58
ico-FL-S2-aptamer-anchor-026	GGTCATAGCATTAGCATTAGCGTCCCAGTAGCGTTGATATTTTGAGAGTTAGGAATGT	58
ico-FL-S2-aptamer-anchor-027	CCCCTGCCTGAATTTAGTGCCTTGTGGAAAGCACCACCGGTTTGAGAGTTAGGAATGT	58
ico-FL-S2-aptamer-anchor-028	ACGGAATAATAATAAGCAAAGTTACCACCACCCTCAGAGCTTTGAGAGTTAGGAATGT	58
ico-FL-S2-aptamer-anchor-029	CCTTTACACGCTAACGAACGATTTTCCTGAATAGAAAATATTTGAGAGTTAGGAATGT	58
ico-FL-S2-aptamer-anchor-030	ACCGTCACCACAATCAAAATATTGAATAAGTTAGAAGGCTTTTGAGAGTTAGGAATGT	58
anti-ico-FL-S2-aptamer	CATATCCGCGTCGCTGCGCTCAGACCCACCACCACGCACCACATTCCTAACTCTCAAA	58